Quaternary Science Reviews 227 (2020) 106044

Contents lists available at ScienceDirect

Quaternary Science Reviews

journal homepage: www.elsevier.com/locate/quascirev

Insights into the evolution of the young Lake Ohrid ecosystem and vegetation succession from a southern European refugium during the Early Pleistocene

Konstantinos Panagiotopoulos [a, *], Jens Holtvoeth [b, c], Katerina Kouli [d], Elena Marinova [e, f], Alexander Francke [g], Aleksandra Cvetkoska [h], Elena Jovanovska [i], Jack H. Lacey [j], Emma T. Lyons [b], Connie Buckel [b], Adele Bertini [k], Timme Donders [l], Janna Just [m], Niklas Leicher [a], Melanie J. Leng [j, n], Martin Melles [a], Richard D. Pancost [b, c], Laura Sadori [o], Paul Tauber [a], Hendrik Vogel [p], Bernd Wagner [a], Thomas Wilke [i]

[a] Institute of Geology and Mineralogy, University of Cologne, Zülpicher Str. 49a, 50674, Cologne, Germany
[b] School of Chemistry - Organic Geochemistry Unit, University of Bristol, Cantocks Close, Bristol, BS8 1TS, United Kingdom
[c] School of Earth Sciences, University of Bristol, Queens Road, Bristol, BS8 1RJ, United Kingdom
[d] Faculty of Geology and Geoenvironment, National and Kapodistrian University of Athens, Athens, Greece
[e] Landesamt für Denkmalpflege am Regierungspräsidium Stuttgart, Referat 84.1/ Archäobotanik, Fischersteig 9, 78343, Gaienhofen-Hemmenhofen, Germany
[f] Institute for Archaeological Sciences, Archaeobotany Workgroup, University of Tübingen, Rümelinstraße 23, 72072, Tübingen, Germany
[g] School of Earth, Atmospheric, and Life Science, University of Wollongong, Wollongong, Australia
[h] Department of Aquatic Ecology, Netherlands Institute of Ecology (NIOO-KNAW), Wageningen, the Netherlands
[i] Department of Animal Ecology & Systematics, Justus Liebig University Giessen, Giessen, Germany
[j] National Environmental Isotope Facility, British Geological Survey, Nottingham, UK
[k] Dipartimento di Scienze della Terra, Università di Firenze, Firenze, Italy
[l] Palaeoecology, Department of Physical Geography, Utrecht University, Utrecht, the Netherlands
[m] Fachbereich Geowissenschaften, Universität Bremen, Bremen, Germany
[n] Centre for Environmental Geochemistry, School of Biosciences, University of Nottingham, UK
[o] Dipartimento di Biologia Ambientale, Università di Roma "La Sapienza", Rome, Italy
[p] Institute of Geological Sciences & Oeschger Centre for Climate Change Research, University of Bern, Bern, Switzerland

ARTICLE INFO

Article history:
Received 31 July 2019
Received in revised form
25 October 2019
Accepted 30 October 2019
Available online xxx

Keywords:
Mediterranean region
Mid-altitude refugium
Relicts
Vegetation succession
Pollen-based biome reconstruction
Palynological richness
Microscopic charcoal
Lipid biomarkers
Diatoms
Stable isotopes

ABSTRACT

Mediterranean mid-altitude sites are critical for the survival of plant species allowing for elevational vegetation shifts in response to high-amplitude climate variability. Pollen records from the southern Balkans have underlined the importance of the region in preserving plant diversity over at least the last half a million years. So far, there are no records of vegetation and climate dynamics from Balkan refugia with an Early Pleistocene age. Here we present a unique palynological archive from such a refugium, the Lake Ohrid basin, recording continuously floristic diversity and vegetation succession under obliquity-paced climate oscillations. Palynological data are complemented by biomarker, diatom, carbonate isotope and sedimentological data to identify the mechanisms controlling shifts in the aquatic and terrestrial ecosystems within the lake and its catchment. The study interval encompasses four complete glacial-interglacial cycles (1365–1165 ka; MIS 43–35). Within the first 100 kyr of lake ontogeny, lake size and depth increase before the lake system enters a new equilibrium state as observed in a distinct shift in biotic communities and sediment composition. Several relict tree genera such as *Cedrus*, *Tsuga*, *Carya*, and *Pterocarya* played an important role in ecological succession cycles, while total relict abundance accounts for up to half of the total arboreal vegetation. The most prominent biome during interglacials is cool mixed evergreen needleleaf and deciduous broadleaf forests, while cool evergreen needleleaf forests dominate within glacials. A rather forested landscape with a remarkable plant diversity provide unique insights into Early Pleistocene ecosystem resilience and vegetation dynamics.

* Corresponding author.
E-mail address: panagiotopoulos.k@uni-koeln.de (K. Panagiotopoulos).

https://doi.org/10.1016/j.quascirev.2019.106044

1. Introduction

Our current understanding of Early Pleistocene climate is mostly based on globally distributed marine sediment cores and particularly benthic oxygen isotope records that provide the means to infer ice volume changes (e.g. LR04 stack by Lisiecki and Raymo, 2005). Besides orbital forcing, a long-term cooling trend that began during the Pliocene and continued into the Pleistocene is evident in the global isotope stack and is linked to the intensification of northern hemisphere glaciations (e.g. Maslin et al., 1998). The period from 1.25 Ma to 0.7 Ma marks the transition from 41-kyr to 100-kyr glacial-interglacial cycles during the Middle Pleistocene (Clark et al., 2006). This so-called Early Middle Pleistocene Transition (EMPT) is associated with an increase in global ice volume, in the duration and severity of glaciations, as well as the gradual loss of plant diversity in Europe (e.g. Head and Gibbard, 2015; Magri et al., 2017; Maslin and Ridgwell, 2005).

Although the response of vegetation to climate variability within the 100-kyr cycles of the Late Pleistocene has been relatively well studied from marine and continental archives across the Mediterranean region, little is known by comparison about vegetation and climate dynamics during the Early Pleistocene (2.56–0.78 Ma). Middle and Late Pleistocene pollen records suggest alternating phases of forested landscapes during interglacials and open landscapes during glacials, while millennial climate oscillations are usually recorded in high-resolution records as relatively abrupt shifts in the vegetation (e.g. Altolaguirre et al., 2019; Fletcher et al., 2010; Follieri et al., 1989; Kousis et al., 2018; Koutsodendris et al., 2019; Leroy, 2007; Panagiotopoulos et al., 2014; Sánchez Goñi et al., 2002; Tzedakis et al., 2006). In order to constrain the amplitude and nature of obliquity-paced climate in the Mediterranean region and the Balkan peninsula in particular, there is a need to investigate the response of terrestrial ecosystems to climate oscillations in the 41-kyr world.

One of the major challenges in studying Early Pleistocene vegetation and climate dynamics is the scarcity of records, especially from the Eastern Mediterranean. Most of the Mediterranean pollen records encompassing intervals across the EMPT (1.4–0.4 Ma *sensu* Head and Gibbard, 2015) originate from the Iberian and Italian peninsulas, but they are usually discontinuous (e.g. Bertini, 2001; Joannin et al., 2007; Leroy, 1997, 2008; Ravazzi and Rossignol Strick, 1995; Suc et al., 2010; Toti, 2015). Despite this limitation, the pollen records register high-frequency climate variability that is induced by precessional insolation changes throughout the Pleistocene (e.g. the pollen record of Tenaghi Philippon; Tzedakis et al., 2006). A gradual expansion of open herbaceous vegetation and a parallel decline in forest diversity (i.e. tree species extinctions) over the course of the Early and Middle Pleistocene is also observed (Combourieu-Nebout and Grazzini, 1991; Combourieu-Nebout et al., 2015; Suc, 1984; Tzedakis et al., 2006). During Pleistocene glacials, while large areas of northern Europe were covered by continental ice-sheets, glaciers in the Iberian, Italian and Balkan peninsulas mountain glaciers persisted only at higher elevation and reached their maximum extent in the Middle Pleistocene (Hughes et al., 2006).

Paleobotanical records from the western and central Mediterranean indicate the gradual contraction and extinction of taxa such as *Taxodium*, *Cathaya*, *Sciadopitys*, *Tsuga*, *Cedrus*, *Carya*, *Engelhardia*, *Eucommia*, *Liquidambar*, *Nyssa*, *Parrotia*, *Pterocarya* over the course of the Early Pleistocene (Bertini, 2010; Combourieu-Nebout et al., 2015; Magri and Palombo, 2013; Postigo-Mijarra et al., 2010). Pollen records from the Italian peninsula suggest that these subtropical to (warm) temperate tree species persisted until they became extinct over the course of the EMPT, while their last occurrence is often recorded in southern Italy indicating the presence of tree refugia in the area (Bertini, 2010; Magri et al., 2017). By comparison, the low-altitude pollen record of the Tenaghi Philippon fen (50 m asl) in northeastern Greece shows the last occurrence of *Parthenocissus* and *Liriodendron* prior to the EMPT, *Cedrus, Eucommia, Parrotia*, and *Tsuga* become extinct over the EMPT, while *Carya* and *Pterocarya* populations most likely persisted into the 100-kyr world (Tzedakis et al., 2006; Van Der Wiel and Wijmstra, 1987). These vegetational shifts have been attributed mostly to climate oscillations, catchment dynamics, as well as biogeographical and ecological traits of different plant species (e.g. Bhagwat and Willis, 2008; Svenning, 2003).

Chronostratigraphic correlation of fragmented sediment sequences, even from neighboring sites, is notoriously difficult and local factors influencing the depositional environment cannot always be clearly distinguished from climate forcing (e.g. Fusco, 2010). In comparison, the chronology of marine pollen sequences from the Mediterranean, such as from southern Italian outcrops near Montalbano Jonico and Crotone, is commonly based on stratigraphic correlations of calcareous plankton, stable isotopes and sapropels (Joannin et al., 2007, 2008). These sequences are invaluable for inferring regional paleoclimate, but do not always allow for local vegetation reconstructions as the pollen source area in most marine sites is not that well constrained. The study of long, continuous lacustrine sediment sequences that record environmental changes at a specific site over consecutive climatic cycles can successfully overcome these limitations. Long terrestrial pollen records from southern Europe have been routinely correlated with the marine isotope stage (MIS) stratigraphy that enables the assessment of vegetation and climate dynamics under different boundary conditions (e.g. the Tenaghi Philippon spanning the last 1.35 Ma, Pross et al., 2015; Tzedakis et al., 2006 and references therein). Thus, long continuous pollen records comprising several climatic cycles with well-studied depositional settings are instrumental in improving our understanding of the evolution of Mediterranean flora and climate over the Pleistocene (e.g. De Beaulieu et al., 2001; Sadori et al., 2016; Tzedakis et al., 2006).

There is consequently a need to analyze further continuous archives of Early Pleistocene age from southern Europe to provide a coherent understanding of the evolution of regional flora and relict species extinctions in the Eastern Mediterranean region. The low-altitude Tenaghi Philippon record reaching back to the 41-kyr world is the principal source of continuous vegetation history in the Eastern Mediterranean, but the site most likely experienced migration lags during reforestation phases as glacial tree refugia are not within its direct proximity, and has not been independently dated. Until recently there were no continuous pollen and charcoal records from Mediterranean refugia encompassing the EMPT. In an effort to address this gap and to decipher plant diversity patterns, as well as biome and climate dynamics, in a Mediterranean refugium and modern biodiversity hotspot, we present the first Early Pleistocene (Calabrian) multi-proxy paleoenvironmental record from a mid-altitude Quaternary refugium retrieved as part of the SCOPSCO (Scientific Collaboration On Past Speciation Conditions in Lake Ohrid) deep drilling project carried out at Lake Ohrid in 2013 (Wagner et al., 2014).

In order to better constrain the influence of local factors (such as lake bathymetry and catchment morphology) on the aquatic and terrestrial ecosystem response to climate variability, we integrate palynological, biomarker, diatom, geochemical and sedimentological data to test four hypotheses about the Early Pleistocene (1365–1165 ka; MIS 43–35) paleoenvironments within the Ohrid catchment: (1) Lake Ohrid was a relative shallow and small eutrophic lake, (2) the Ohrid basin fostered a high plant diversity and abundance of relict species, (3) the lower amplitude of climate variability within obliquity-paced climate cycles attenuated

terrestrial and aquatic ecosystem response, and (4) Early Pleistocene climate in the region was warmer and wetter in comparison to the Late Pleistocene.

2. Physical setting

Lake Ohrid (Albania/North Macedonia) is situated at an altitude of 693 m above sea level (asl) and is surrounded by high mountain ranges with several peaks above 2000 m asl (Fig. 1). Lake Ohrid is located in an active tectonic graben that developed during the latter stages of alpine orogeny (Lindhorst et al., 2015). Devonian metasediments occur in the northeastern parts of the basin, Triassic limestones and clastics in the northwest, east and southeast, Jurassic ophiolites in the west, and Quaternary fluvial sediments occupy the plains in the north and south of Lake Ohrid (Hoffmann et al., 2010). Lake Ohrid is rather large (358 km^2), deep (max. 293 m, mean 155 m) and has a total water volume of 55 km^3 (Lindhorst et al., 2015; Matzinger et al., 2007). Inflow from karst aquifers accounts for 55% of the water balance with smaller shares from direct precipitation and river inflow (Matzinger et al., 2006). The karst aquifers are charged by orographic precipitation and from springs derived from Lake Prespa which lies 160 m higher and has no surface outflow. The two lakes are hydrologically connected via underground channels in the Galičica/Mali i Thatë mountains and have a combined catchment area of approximately 2600 km^2 (1300 km^2 excluding Lake Prespa). Drainage by the Crni Drim River and loss by evaporation account for water outflow. Lake Ohrid is oligotrophic and oligomictic with a weak density stratification and complete overturn of the water column occurring on average every few years during cold winters (Matzinger et al., 2007). In constrast, Lake Prespa is eutrophic, rather shallow (max. 55 m, mean 14 m), smaller (254 km^2), with a total water volume of 3.6 km^3 and mixing (convection and wind) occurs annually (Matzinger et al., 2006).

The study region is characterized by a sub-Mediterranean climate with hot and dry summers and cold and wet winters with a mean annual temperature of 11 °C at 760 m asl. Mean annual precipitation measured within the Ohrid catchment increases from 698 mm at 760 m asl to 1194 mm at 975 m asl (Popovska and Bonacci, 2007). The diverse topography of the Lake Ohrid catchment and its location at a transitional climate zone gave rise to an assemblage of central European, Mediterranean and Balkan endemic plant species (Polunin, 1980). The major vegetational belts encountered within the Ohrid and Prespa catchment listed with decreasing altitude are: the alpine and subalpine meadows, the montane conifer forests (notably the endemic *Pinus peuce* forests forming the treeline in the Pelister mountain), the montane deciduous forests (dominated by beech associated with fir forming the treeline in the Galičica/Mali i Thatë mountains), the mixed deciduous oak forests (with thermophilous species closer to the lake) and the grasslands of the littoral zone. Mediterranean elements are mostly confined in the lowlands within the semi-deciduous oak-hornbeam dominated forests (Matevski et al., 2011; Panagiotopoulos, 2013; Sadori et al., 2016).

3. Materials and methods

3.1. Sedimentology and inorganic geochemistry

The interval examined in this study (400–447 m composite depth) comprises hemipelagic deposits, which were classified into three lithotypes based on visual core descriptions and sediment physical properties such as calcite content (Fig. 2; see Francke et al., 2016 for details). The occurrence of coarser sediments and shell fragments below 447 mcd (corresponding to 430 core depth in Wagner et al., 2014) is characteristic of shallow water facies. Sediment recovery from 400 to 447 mcd is 100% and no mass movement deposits are documented.

X-ray fluorescence (XRF) scanning was carried out at 2.5 mm resolution using an ITRAX core scanner (COX analytics, Sweden) equipped with a chromium (Cr) X-ray source set at 30 kV and 30 mA at the Institute of Geology and Mineralogy at the University of Cologne. Elemental analysis was performed at 16 cm intervals

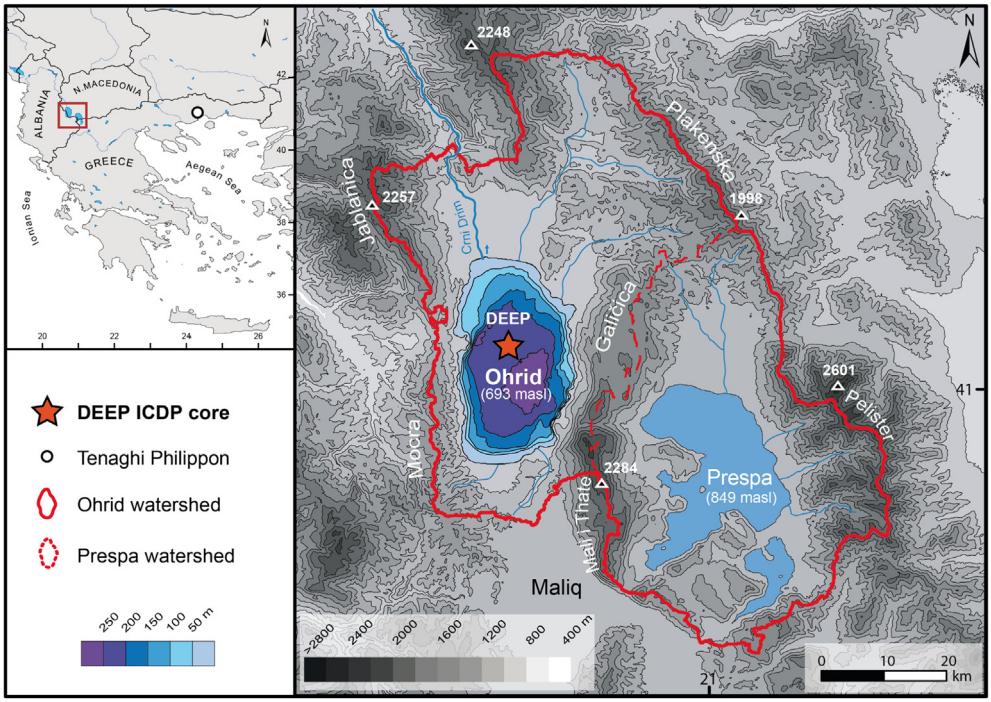

Fig. 1. Lake Ohrid topography and bathymetry (modified after Panagiotopoulos, 2013).

(292 samples, ~686 yr) on freeze-dried and ground (<63 μm) samples. Total carbon (TC) and total inorganic carbon (TIC) were measured after combustion and chemical treatment using a DIMATOC carbon analyzer. The total organic carbon (TOC) content was calculated by subtracting TIC from TC. For grain size samples were taken at 64 cm intervals (73 samples, ~2718 yr) and were analyzed using a BECKMAN-COULTER particle analyzer after chemical treatment to remove any non-detrital matter from the bulk sediment composition (Francke et al., 2016 for more details). Samples were mixed with Gramham's salt and sonicated for 1 min prior to analyses to prevent formation of clay aggregates. Biogenic silica (BSi) was determined at 32 cm resolution (146 samples, ~364 yr) by means of Fourier transform infrared spectroscopy (Vogel et al., 2016 and references therein) at the Institute of Geological Sciences at the University of Bern.

Oxygen and carbon isotopes were measured on bulk carbonate (calcite) samples at 16 cm resolution (182 samples) throughout intervals with a higher carbonate content (>0.5%) at the British Geological Survey following the same analytical protocol detailed by Lacey et al. (2016). The oxygen and carbon isotope composition of calcite ($\delta^{18}O_c$ and $\delta^{13}C_c$) are reported in standard delta notation in per mille (‰) calculated to the Vienna Pee Dee Belemnite scale using within-run laboratory standards calibrated against international NBS standards. Analytical reproducibility for the reference materials was <0.1‰ ($\pm 1\sigma$) for $\delta^{18}O$ and $\delta^{13}C$.

3.2. Chronology

The chronology of the study interval (400–447 mcd) is based on the age-depth model for the entire DEEP site sequence, which uses tephrochronological information as first-order tie points supplemented by second-order tie points derived from tuning of climate-sensitive proxy data against orbital parameters (Wagner et al., 2019). For the study interval (1165–1365 ka), the chronology is based solely on orbital tuning of total organic carbon content (assuming that total inorganic carbon maxima represent interglacial periods) and the tie points obtained are shown in Fig. 3. During these first 200 kyr sedimentation rates vary from 0.042 to 0.008 (average of 0.027 cm yr^{-1}). All ages are reported in calibrated kiloyears before present (ka).

Two tephra layers (OH-DP-4089 at 408.98 mcd and OH-DP-4124 at 412.42 mcd) encountered within the study interval represent so far unknown eruptions of the incompletely understood Early Pleistocene Italian volcanism. The occurrence of ferrimagnetic sulphides during glacials overprints the primary detrital magnetic signal (Just et al., 2016; in review) complicating the interpretation of the paleomagnetic data. Nevertheless, anomalous inclinations carried by (early) diagenetic greigite are evident at 420 mcd and between 410 and 405 mcd and based on the orbitally-tuned age model could correspond to Bjorn and Cobb Mountain excursions (Just et al., in review). Thus, the base of the Jaramillo sub-Chron at 373.8 mcd (1072 ka according to the age model) is the lowermost independent chronostratigraphic marker used for cross-evaluation of the orbitally-tuned lower part of the sequence (Wagner et al., 2019).

3.3. Palynology and biome reconstruction

Palynological analysis was performed at the Institute of Geology and Mineralogy at the University of Cologne (Germany) on 103 samples down to 16 cm intervals. This increases the temporal resolution of the skeleton pollen record of the Lake Ohrid DEEP core (from approximately 3130 years for the 73 samples spaced at 64 cm sampling intervals; Wagner et al., 2019) to 1945 years for the study interval (400–447 mcd). Dry sediment samples were weighted, spiked with two *Lycopodium* spore tablets (18583 spores/tablet) to allow for calculation of palynomorph concentrations, and treated with HCl (37%), HF (40%) and NaOH (10%). Palynomorphs were identified to the lowest taxonomical level under 400× and 630× magnification. An average pollen sum of 998 (515) terrestrial pollen grains excluding (*Pinus*), spores, obligate aquatics, and algae were counted per sample to ensure recording of rare pollen taxa in specific relict species. Consequently, ten skeleton samples (64 cm resolution) analyzed within the Lake Ohrid Palynological group between 435.12 and 440.08 mcd (1318.15–1348.15 ka) were reprocessed and recounted. Pollen relative percentages of terrestrial vascular plants were calculated upon this sum.

Palynomorphs were identified with the help of reference collection material at the University of Cologne and pollen atlases (Beug, 2004; Reille, 1992, 1995, 1998). For bisaccate pollen grains, the keys of Liu and Basinger (2000) and Zanni and Ravazzi (2007) were also consulted. Pines are included in the pollen sum as they were not found to be overrepresented in the Early Pleistocene pollen spectra (greater than 50% and 70% in 39 samples and 13 samples respectively). However, to facilitate comparability with published pollen records from younger Pleistocene intervals from the DEEP site (e.g. Sadori et al., 2016; Wagner et al., 2019), selected pollen percentage groups are also presented excluding *Pinus* (Fig. 3).

Diploxylon pines (*Pinus sylvestris*-type) were differentiated from haploxylon ones (*P. peuce*-type) that are well-adapted to subalpine climate conditions and form the modern treeline in parts of the catchment (Fig. 4; Panagiotopoulos, 2013). Cupressaceae comprises differentiated inaperturate grains with (*Taxodium*-type) and without papilla. *Quercus* comprises differentiated deciduous (*Q. robur*-type and *Q. cerris*-type) and evergreen types. Ecological groups include the following taxa: montane (*Abies, Betula, Fagus, Cathaya, Cedrus, Picea* cf. *abies*, *Picea* cf. *omorika*, *Pinus peuce*-type, *Taxus,* and *Tsuga*) and mesophilous (*Acer, Buxus, Carpinus betulus, Castanea, Carya, Celtis, Corylus, Distylium, Engelhardia, Eucommia, Fraxinus excelsior,* Hammamelidaceae, *Ostrya/Carpinus orientalis, Parrotia, Parthenocissus, Platanus, Pterocarya, Hedera, Quercus robur*-type, *Quercus cerris*-type, *Tilia, Ulmus,* and *Zelkova*). Asteroideae comprise differentiated *Anthemis*-, *Cirsium*-, and *Senecio*-types. Poaceae includes grass grains smaller and greater than 40 μm. *Phragmites* pollen grains were not differentiated and are included in the Poaceae (wild type) group (see also Panagiotopoulos et al., 2014). Aquatic vascular plants comprise differentiated *Lemna*, *Myriophyllum*, *Nuphar*, *Nymphaea*, *Potamogeton*, *Sparganium*-type, *Typha latifolia*-type. *Pediastrum* comprising *P. boryanum* and *P. simplex* are freshwater planktonic green algae, which have a cosmopolitan distribution and wide ecological tolerance (Komárek and Jankovská, 2001). Both species are typically dominant in eutrophic lakes under temperate climates, although the latter is also commonly found in tropical regions (Komárek and Jankovská, 2001). The synchronous occurrence of *Botryococcus* (mostly *B. braunii*) and *Pediastrum* species is characteristic of eutrophic lakes with large extent of open central areas and extensive submerged and littoral vegetation typical for climatic optima (Jankovská and Komárek, 2000).

Palynological richness was determined in 99 samples (four samples with a main pollen sum of less than 400 grains were left out of the analysis) with a standard pollen sum of 400 terrestrial grains, $E(T_{400})$, using PSIMPOLL (Bennett, 2008, Fig. 5). Rarefaction analysis provides minimum variance unbiased estimates of the expected number of taxa (t) in a random sample of n individuals taken from a collection of N individuals containing T taxa (Birks and Line, 1992). Consequently, it enables comparison of richness between samples of different size by standardizing pollen counts to a single sum. The expected number of taxa, $E(T_n)$, for each sample is

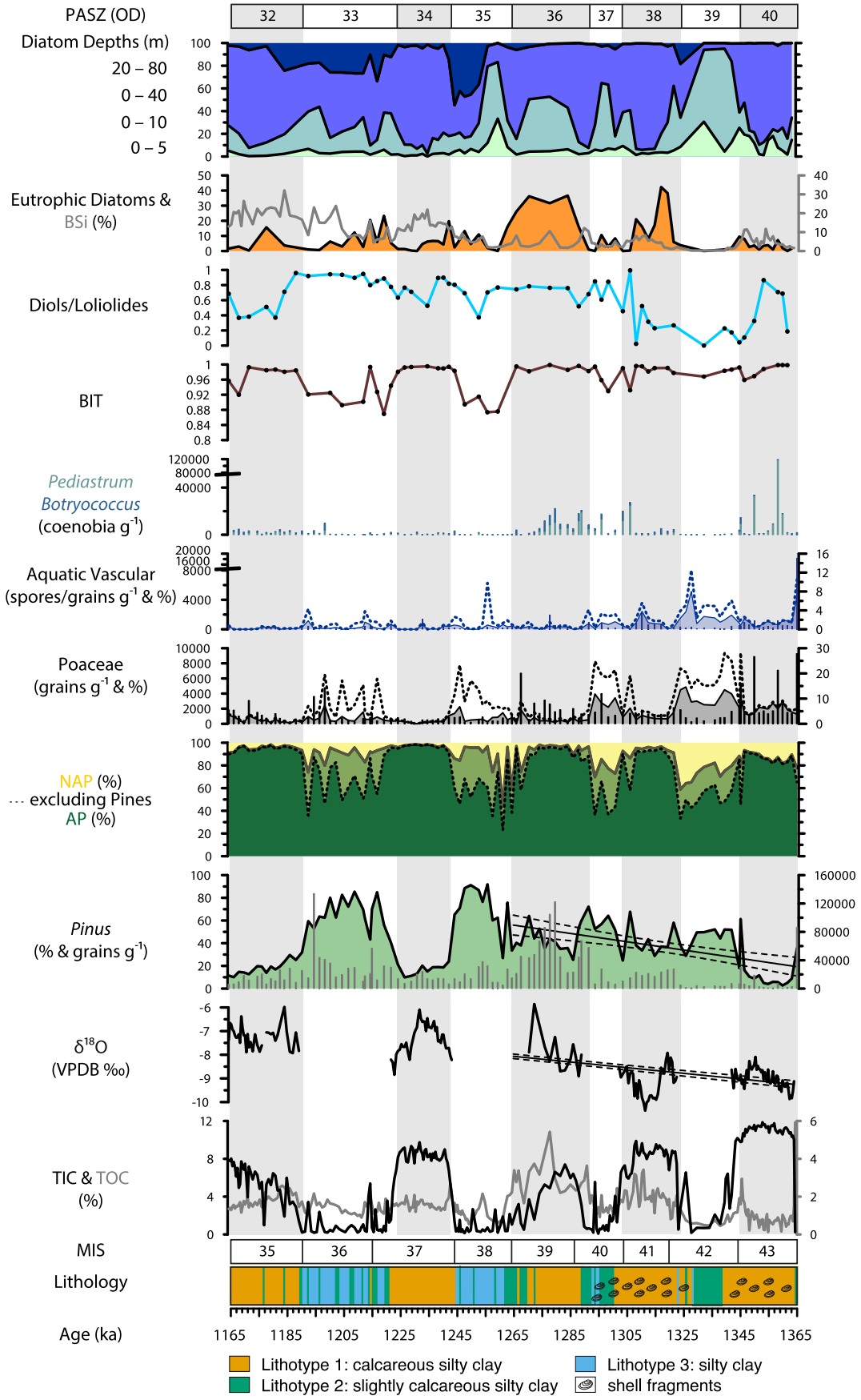

Fig. 2. Lake Ohrid palynological, biomarker, diatom, and geochemical data plotted against age. Lithology; marine isotope stages from the LR04 benthic isotope stack (Lisiecki and Raymo, 2005); total inorganic and organic carbon; bulk carbonate oxygen isotopes; pines, arboreal/non arboreal, Poaceae, aquatic vascular percentages and concentrations (dashed lines with pines excluded from the pollen sum), green algae concentrations; BIT index; diols (eustigmatophytes)/loliolides(diatoms); eutrophic diatom; BSi; diatoms grouped after habitat preferences. Gray bars show interglacial intervals based on CONNISS zoning results. (For interpretation of the references to color in this figure legend, the reader is referred to the Web version of this article.)

based on a common value of n, usually the smallest total count in the samples to be compared, and the rarefied sample will thus contain $t \leq T$ taxa and consist of $n \leq N$ (*cf.* Birks and Line, 1992). Palynological richness can be used to infer floristic diversity (species richness) in the pollen source area. However, it does not address the question of species evenness (relative frequency of taxa) and is influenced by factors affecting pollen dispersal. Thus, herbaceous pollen is usually underrepresented in forested stages due to limited wind dispersal below the canopy (Birks and Line, 1992). Considering the size of the basin, the curve of $E(T_{400})$ at Ohrid most likely captures changes in taxonomic richness at a landscape scale (γ-diversity *sensu* Whittaker, 1972) and is influenced by climate, vegetation succession, and disturbance events (e.g. fire and lake-level change).

We applied the biomization method developed by Prentice et al. (1992) to fossil pollen data from the Lake Ohrid DEEP to reconstruct the distribution of Early Pleistocene biomes. This method assigns the pollen taxa to plant functional types (PFTs) and to major vegetation types (biomes) on the basis of plant ecology and biology, bioclimatic tolerance and spatial distribution of pollen-producing plants (Prentice et al., 1992, 1996). This method has been tested using extensive surface pollen datasets and regionally adapted biome-taxa matrixes (e.g. Europe, Prentice et al., 1996). Here we use the regionally adapted biome-taxa matrix of Marinova et al. (2018) developed for the Eastern Mediterranean-Black Sea-Caspian-Corridor (EMBSeC). All terrestrial pollen taxa identified in the Early Pleistocene pollen spectra of the Lake Ohrid DEEP core analyzed in this study were assigned to twenty-four plant functional types and to thirteen biomes as defined for the region (Marinova et al., 2018). Relict plant genera and families (i.e. *Cathaya, Engelhardia, Eucommia,* Hamamelidaceae, *Parrotia,* and *Tsuga*) currently not encountered in modern day vegetation of the aforementioned EMBSeC region, but present in the fossil pollen spectra of Lake Ohrid DEEP (with abundances greater than 0.5%) were assigned based on their modern bioclimatic traits and natural distribution to the following PFTs: cool-temperate evergreen needleleaved tree (*Tsuga*), temperate evergreen needleleaved tree (*Cathaya, Tsuga*), temperate (spring frost intolerant) cold-deciduous malacophyll broadleaved tree (*Engelhardia*, *Eucommia*, Hamamelidaceae, *Parrotia*), temperate low to high shrub (Hamamelidaceae), warm-temperate evergreen malacophyll broadleaved tree (Hamamelidaceae).

3.4. Lipid biomarkers

A total of 55 biomarker samples down to 64 cm intervals with an average temporal resolution of 3580 years were analyzed at the University of Bristol for their biomarker composition, in particular, alkyl lipids (*n*-alkanes, *n*-fatty acids, *n*-alcohols, and related compounds) and glycerol-dialkyl-glycerol-tetraethers (GDGTs) distributions. Microwave-assisted solvent extraction was used to retrieve total lipid extracts (TLEs) containing both alkyl lipids and GDGTs (solvents: dichloromethane/methanol 2:1, v:v; heating to 70 °C at 5 °C/min, holding at 70 °C for 10 min). Aliquots of the TLEs were prepared for total lipid analysis by gas chromatography-mass spectrometry (GC-MS) and for GDGT analysis by ultrahigh-performance liquid chromatography/atmospheric pressure chemical ionization−mass spectrometry (UHPLC/APCI-MS).

For total lipid analysis, dried TLEs were treated with methanol/acetyl chloride (30:1, v:v; 12 h at 45 °C) to break up ester bonds and transmethylate fatty acids (acid-catalyzed one-step saponification and methylation). After removal of excess mineral acids with potassium carbonate and drying of the TLEs, N,O-bis-(trimethylsilyl)-trifluoroacetamide (BSTFA, 45 min at 65 °C) was added for the derivatization of hydroxy groups, e.g., in alcohols, sterols or hydroxy acids. The TLEs were then analyzed using a Thermo Scientific Trace 1300 GC connected to a Thermo Scientific ISQ LT Single Quadrupole Mass Spectrometer (GC column: Agilent HP-1, 50 m × 0.32 mm x 17 μm; temperature program: 60 °C, held for 1 min, heating at 6 °C/min to 170 °C, then 2.5 °C/min to 315 °C, held for 10 min). Compounds were identified through their mass spectrum and retention order and quantified relative to an internal standard (5α-cholestane) added prior to extraction.

For GDGT analysis, TLE aliquots were separated into polar and apolar fractions using short alumina columns, with the apolar fraction eluted with *n*-hexane/DCM 9:1 (v:v) and the polar fraction eluted with dichloromethane/methanol 2:1 (v:v). The polar fraction was then filtered (syringe filters; solvents: *n*-hexane/*iso*-propanol 99:1, v:v) and analyzed in duplicate, using a ThermoFisher Scientific TSQ Quantum Access, fitted with a ThermoFisher Scientific Accela PDA Detector. Two Waters Acquity UPLC BEH Hilic columns (2.1 mm × 150 mm x 1.7 μm) were operated with an isocratic flow rate of 0.2 mL/min to attain normal phase separation. Samples were eluted for 25 min with 82% hexane and 18% *n*-hexane/*iso*-propanol 9:1, then the proportion of *n*-hexane/*iso*-propanol 9:1 was increased linearly to 35% over 25 min, and then to 100% over 30 min. Selective ion monitoring mode (SIM) was used for heightened sensitivity and the data were analyzed from the $[M+H]^+$ peaks of the individual GDGTs.

3.5. Diatoms

Diatom analyses was performed on 68 samples with an average temporal resolution of 2918 years (down to 64 cm intervals) at the University of Giessen and the University of Utrecht. Dry sediment samples were treated with H_2O_2 (35%) and HCl (10%). An average of 290 diatom valves was identified and counted at 1500× magnification. Diatom identification follows Levkov et al. (2007), Cvetkoska et al. (2014), Jovanovska et al. (2016) and references therein. Diatom counts were converted to relative percentages using TILIA (Grimm, 1992) and grouped according to their ecological and habitat preferences. The diatom group indicating eutrophic conditions comprises *Aulacoseira ambigua, A. granulata, Ulnaria biceps*, and *U. acus.* Diatom taxa were also categorized in five depth classes according to their habitat preferences and spatial distribution in the lake: 0−5 m (shallow littoral communities), 0−10 m (littoral communities), 0−40 m (epilimnetic planktonic and sublittoral communities), and 20−80 m (hypolimnetic planktonic communities).

4. Results

4.1. Sedimentology and inorganic geochemistry

Lithotype 1 (calcareous silty clay) dominate interglacial intervals and lithotypes 2 and 3 (slightly calcareous silty clay and silty clay) dominate transitional and glacial intervals (Fig. 2). Lithotype 1 sediments are characterized by high TIC (2−11.6%; mean 7.7%), TOC (0.1−5.4%; mean 1.6%), BSi (0.18−26.5%; mean 8.87%), and low Ti/K values (0−0.49; mean 0.2). Lithotype 2 sediments are characterized by relatively low TIC (0.2−2%; mean 0.96%), TOC (0.4−3.7%; mean 1.5%), BSi (0.26−32%; mean 7.5%), and relatively high Ti/K (0.41−0.51; mean 0.46). Lithotype 3 sediments are characterized by relatively low TIC (<0.5%; mean 0.29%), TOC (0.5−5.9%; mean 1.4%), BSi (0.26−23%; mean 7.6%), and relatively high Ti/K (0.37−0.49; mean 0.46). $\delta^{13}C_c$ vary between −3.2‰ and 0.1‰ (mean −1.5‰) and, with the exception of the first interglacial, an upcore shift to higher $\delta^{13}C_c$ can be observed (Fig. 3). $\delta^{18}O_c$ range between −10.4‰ and −5.9‰ (mean −8.2‰) and an overall shift towards higher $\delta^{18}O_c$ upcore is visible (Fig. 2).

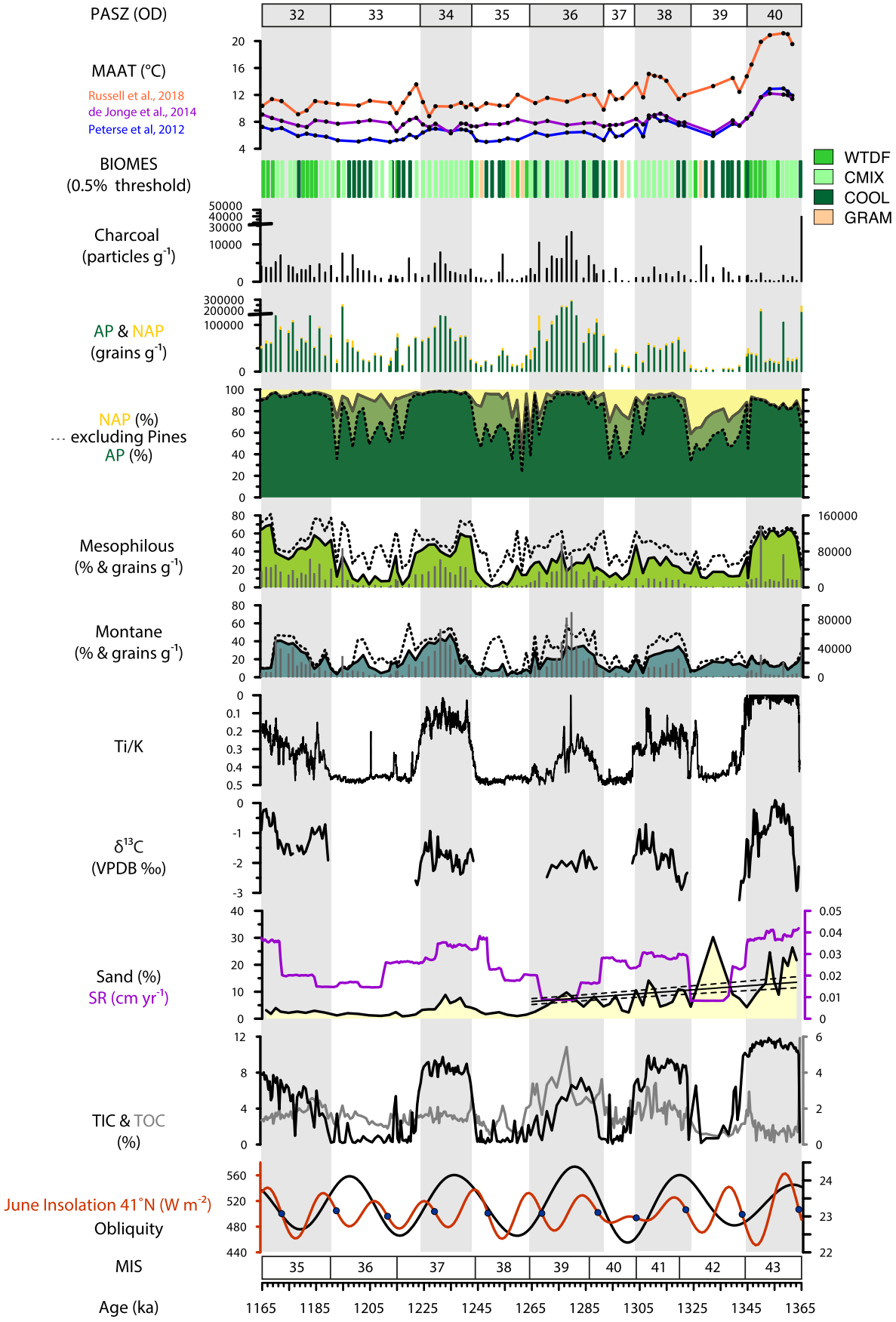

Fig. 3. Ohrid catchment palynological, biomarker, geochemical and biomes data plotted with orbital parameters against age. Obliquity and 21st June insolation at 41 °N (Laskar et al., 2004) with second-order tuning points marked with blue dots (Wagner et al., 2019), marine isotope stages from the LR04 benthic isotope stack (Lisiecki and Raymo, 2005); total inorganic and organic carbon; sand and sedimentation rates; bulk carbonate carbon isotopes; Ti/K; montane, mesophilous, arboreal/non arboreal percentages and concentrations (dashed lines with pines excluded from the pollen sum); microscopic charcoal concentrations (>10 μm); reconstructed biomes; and biomarker-based mean annual air temperature (MAAT) reconstruction. Gray bars show interglacial intervals based on CONISS zoning results. (For interpretation of the references to color in this figure legend, the reader is referred to the Web version of this article.)

4.2. Pollen assemblage superzones

Nine pollen assemblage superzones (PASZ; Ohrid DEEP (OD)-40 to OD-32) were determined with cluster analysis for pollen taxa with a relative abundance greater than 2% using CONISS within the TILIA software (Grimm, 1992, Fig. 5). A total of 118 terrestrial pollen taxa (65 trees, shrubs and vines and 53 upland herbs) were identified. Relict pollen taxa (16 trees, shrubs and vines and 1 upland herb) formed significant constituents of the Calabrian vegetation at Ohrid (up to 48%; Fig. 5), but gradually became extinct over the course of the Pleistocene and are not present in the modern day flora of the region (Sadori et al., 2016; Kousis et al., 2018; Sinopoli et al., 2018). Evenly numbered PASZ are characterized by high mean arboreal pollen abundances and concentrations suggesting 'interglacial' conditions (greater than 87% and 50×10^3 grains g^{-1}), while odd numbered PASZ have lower arboreal pollen abundances and concentrations suggesting 'glacial' conditions (greater than 74% and 11×10^3 grains g^{-1}). Mean PASZ duration based on our chronology is 21.3 kyr that corresponds to half an obliquity cycle (41 kyr). Besides obliquity-paced shifts in ecosystem dynamics at Ohrid, higher frequency shifts in vegetation cover and ecosystem productivity are also visible in the pollen and geochemical records (Fig. 3). Major shifts in individual pollen taxa and ecological group percentages are summarized in Table 1.

4.3. Reconstructed biomes and palynological richness estimates

The biomization method applied to Lake Ohrid DEEP pollen spectra yielded four reconstructed biomes shown in Figs. 3 and 4: warm-temperate deciduous malacophyll broadleaf forest (WTDF), cool mixed evergreen needleleaf and deciduous broadleaf forest (CMIX), the cool evergreen needleleaf forest (COOL), and graminoids with forbs (GRAM). The most frequently reconstructed biome (47 samples; 36 in interglacials/even-numbered PASZ) during the Early Pleistocene at Ohrid is the CMIX biome, followed by the COOL biome (32 samples; 12 in interglacials), the WTDF (19 samples; 13 in interglacials), and GRAM (5 samples in glacials).

Rarefaction analysis was used to estimate palynological richness, $E(T_{400})$, in 99 pollen spectra of the Lake Ohrid DEEP core at a fixed sum of 400 terrestrial pollen grains (four samples in OD 39 with a pollen sum below 400 were excluded). The highest palynological richness is recorded durging the first climatic cycle (1365–1325 ka; MIS 43–42; OD 40–39) and correspond with high herbaceous pollen percentages (Figs. 2 and 3). A distinct period of low $E(T_{400})$ values is recorded at 1250 ka (MIS 38; OD 35) and arboreal percentages are dominated by pines (90%).

4.4. Lipid biomarker composition

The main compound classes quantified from TLE analysis are: *n*-fatty acids (FA; 21% of the total lipids on average), *n*-alcohols (OH, 18 $\%_{lipids}$), hydroxy acids (OH-FA, 11$\%_{lipids}$), sterols (19$\%_{lipids}$), and *n*-alkanes (5$\%_{lipids}$). The remaining 26% are dominated by hopanoic acids (14$\%_{lipids}$) from *in situ* bacterial biomass and long-chain (C_{30}, C_{32}) diols (5$\%_{lipids}$), likely from eustigmatophytes (microalgae; Volkman et al., 1999). Notable other compounds include loliolide and *iso*-loliolide, which are prominent fragments of fucoxanthine, the main pigment in diatoms but also occurring in dinoflagellates and haptophytes (Repeta and Gagosian, 1982; Klok et al., 1984). These compounds show significant variability in abundance (<0.1$\%_{lipids}$ - 13$\%_{lipids}$), especially relative to the diols, thus, indicating changes in the algal community.

In contrast to the Late Pleistocene, the overall lipid composition does not change significantly between glacials and interglacials (Fig. 6; Holtvoeth et al., 2017). However, the proportion of

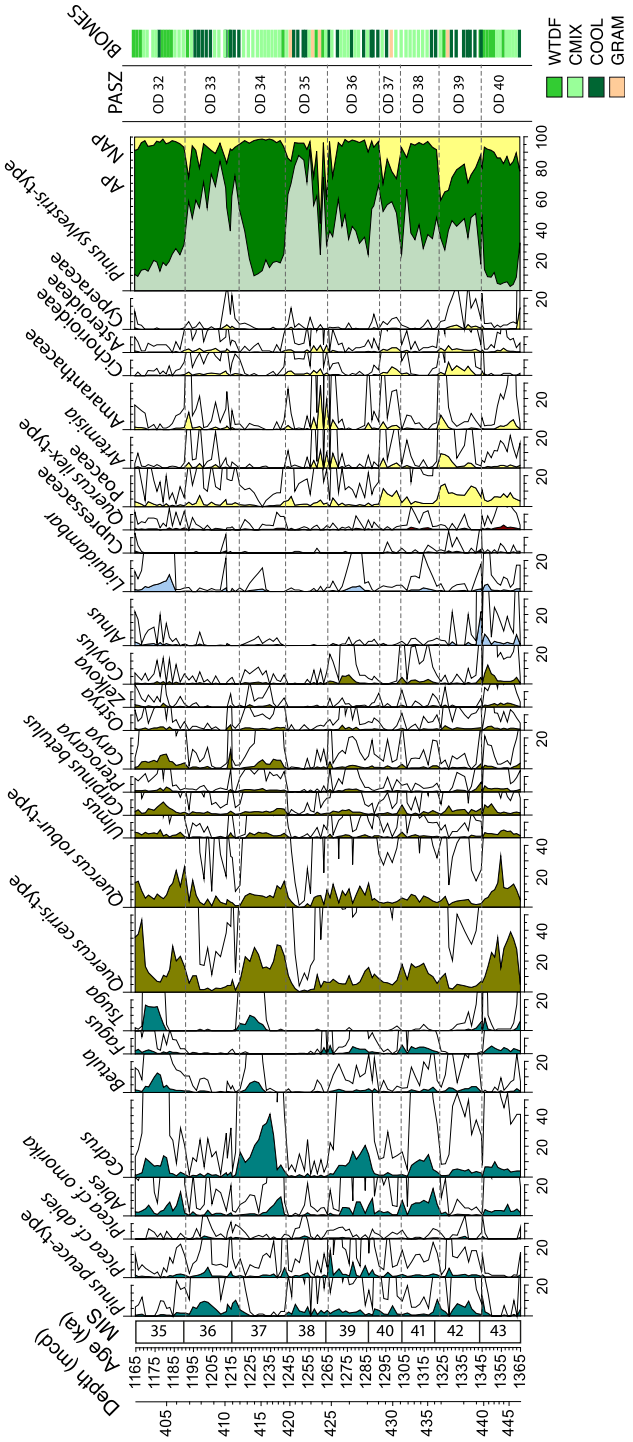

Fig. 4. Lake Ohrid DEEP pollen percentage diagram of selected (>2%) terrestrial taxa (with x 10 exaggeration). Species are color-coded in montane (teal), mesophilous (olive), riparian (blue), Mediterranean (red), herbs (yellow). Marine isotope stages (MIS), pollen assemblage superzones (PASZ), and reconstructed biomes (see Section 3.3 for details) are shown. (For interpretation of the references to color in this figure legend, the reader is referred to the Web version of this article.)

biomarkers from aquatic sources such as long-chain diols and loliode/*iso*-loliolide is significantly higher than in the Late Pleistocene, implying that Lake Ohrid was more productive during the early stages of lake basin development. The diol/loliolide ratio, reflecting changing relative contributions from eustigmatophytes and diatoms, increases with time such that the eustigmatophyte-

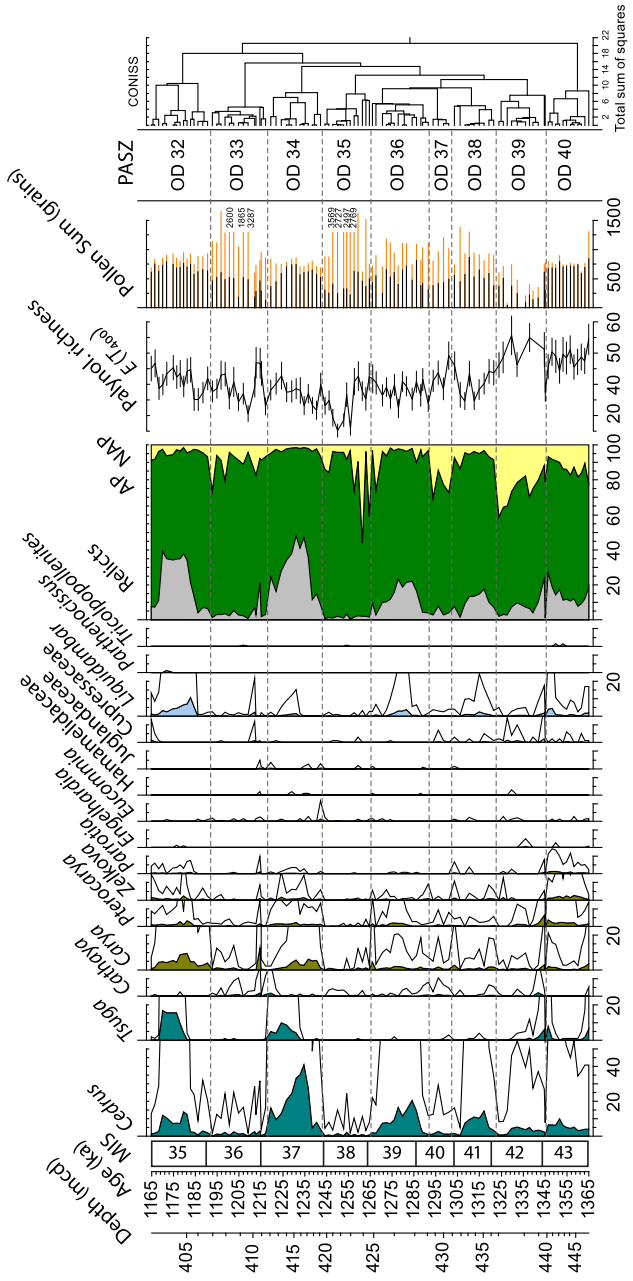

Fig. 5. Lake Ohrid DEEP pollen percentage diagram of relict species (with x 10 exaggeration). Marine isotope stages (MIS), expected number of pollen taxa $E(T_{400})$ with 95% confidence intervals, pollen sum (including pines in orange), pollen assemblage superzones (PASZ), and CONISS are shown. (For interpretation of the references to color in this figure legend, the reader is referred to the Web version of this article.)

derived diols dominate in the later phases of lake development (Fig. 3). Another noteworthy feature of the biomarker record is the uniquely high proportion of C_{23} *n*-alkane in one sample from 1277 ka. This compound is widely interpreted as a biomarker for *Sphagnum* mosses (e.g., Bush and Mcinerney, 2013), a prominent peat moss in wetlands. The peak in the *Sphagnum* marker coincides with peaks in charcoal and the Ti/K ratio as well as the highest TOC value (5.4%) of the entire DEEP Site sedimentary record, suggesting a one-off temporary supply of material from organic-rich wetland soils.

The ratio of branched GDGTs (brGDGTs) over isoprenoid GDGTs (iGDGTs), the so-called BIT index, has been suggested to reflect relative changes in the input of GDGTs from aquatic and soil microbial sources, based on the finding that brGDGTs occur in soils while iGDGTs are produced mainly by aquatic Thamarchaeota (Hopmans et al., 2004; Weijers et al., 2006). There are hardly any isoprenoid GDGTs present in the Early Pleistocene Lake Ohrid DEEP samples, leading to BIT values above 0.85, i.e. the GDGTs appear overwhelmingly of soil bacterial origin (Fig. 2). However, a more recent study by Weber et al. (2015) on a Swiss alpine lake demonstrated that substantial amounts of brGDGTs can also be produced by heterotrophs in the water column. Thus, a change in the BIT index may also indicate a change in the aquatic microbial community. The low abundance of iGDGTs rules out the application of the tetraether index (TEX_{86}), which is a temperature-sensitive ratio of certain iGDGTs and has been applied successfully to Late Pleistocene Lake Ohrid sediments to reconstruct changes in surface water temperature (Holtvoeth et al., 2017). However, a similar approach can be applied to brGDGTs under the assumption that they originate mainly from soil bacteria as their distributions are strongly influenced by soil temperature (Weijers et al., 2007), which closely correlates to air temperature. In an attempt to reconstruct the mean annual air temperature (MAAT), we applied three calibrations to the brGDGT distributions determined in the study interval that are based on the correlation of brGDGT ratios found in global soils (Peterse et al., 2012; De Jonge et al., 2014) and lake sediments (Russell et al., 2018) with the equivalent local MAAT. MAAT values based on the soil calibrations (Peterse et al., 2012; De Jonge et al., 2014) are lower than could be expected for most of the record (OD 39–32: 6–9 °C) with the exception of OD 40 (12 °C, on average). The absolute values from the lake sediment calibration appear more realistic (OD 39–32: 9–15 °C), with OD 40 producing the unlikely outlier values (average of 20 °C), in this case. All three records show a distinct decreasing trend from OD 40 to 37 or 36 and a pronounced cyclicity until OD 37 while only the record based on the calibration by Peterse et al. (2012) shows a glacial interglacial pattern and, in fact, a strong correlation with the TIC record throughout the profile (Fig. 3).

4.5. Diatom indicators of water depth and trophic status

The maximum abundance of eutrophic diatoms occurs at 1317 ka (42.3%) and a prolonged phase of high abundances occurs between 1285 and 1266 ka (with values above 26%; Fig. 2). In the younger half of the study interval (1265–1165 ka) eutrophic diatom percentages remain relatively low (maximum 23.3%). Diatom-inferred lake depth also shows an increase of diatoms favoring habitats with a depth greater than 20 m (i.e. pelagic) in the younger half of the record, whereas diatoms occurring in shallower habitats (e.g. benthic-littoral taxa) dominate the older half (1365–1165 ka; Fig. 2).

5. Discussion

5.1. Lake basin evolution and aquatic ecosystem response

The study interval spans the onset of continuous lacustrine sedimentation at 1365 ka (MIS 43) until 1165 ka (MIS 35), comprising four complete glacial-interglacial cycles, and is divided into nine pollen assemblage superzones (OD 40 – OD 32) with an average PASZ duration of 21.3 kyr reflecting an obliquity-paced climate regime. Discontinuous lacustrine/fluvial sediments encountered downcore (below 447 mcd of the Lake Ohrid DEEP core) with an age greater than 1365 ka (older than the study interval) point to the existence of riverine and peatland habitats before the infilling of the Lake Ohrid basin (Wagner et al., 2014) and are not part of this study.

Table 1
Description of major shifts in pollen, lithology and geochemistry within the pollen assemblage superzones (PASZ) of the Ohrid DEEP (OD) core and inferred paleoenvironment.

PASZ (m, ka cal BP)	Lithology & Geochemistry	Palynomorphs	Inferred paleoenvironment
OD 32 (400.56–406.64 m, 1165–1190 ka); mean pollen sum: 846 (685 excl. Pines)	low sand %, high and fluctuating (increasing) TOC (TIC) & $\delta^{18}O$	AP > 90% (mean 95%), *Quercus* dominant (max 57.9%); high AP conc. (mean 79 × 10^3 grains g^{-1}); max mesophilous 70% (mean 48.5%), max *Q. cerris (*47%), max *Q. robur* (26.6%), max *Carya* (9.6%), max *Carpinus betulus* (8.4%); max montane 41% (mean 23%), max *Tsuga* (16.8%), max *Abies (*15.6%), max *Cedrus* (14.1%), max *Betula* (12.6%); max mediterranean 1.4% (mean 0.7%); max riparian 11.3% (mean 4.5%), max *Liquidambar* (10.8%)	closed evergreen and mixed forests in the montane zone, deciduous forests with thermophilous species, extensive riparian forests
OD 33 (406.96–411.44 m, 1191–1217 ka); mean pollen sum: 1377 (400 excl. Pines)	low sand %, low and fluctuating TIC & TOC	AP > 74% (mean 89%), *Pinus sylvestris* dominant (max 84.3%); relative high AP conc. (mean 50 × 10^3 grains g^{-1}); max mesophilous 35% (mean 14.1%); max montane 24.7% (mean 12.1%), max *Pinus peuce* (10.3%); max mediterranean 0.8% (mean 0.2%); max riparian 3.4% (mean 0.4%); max Amaranthaceae (11.5%)	Pine forests dominant associated with montane tree stands, mesophilous tree stands and grasslands in the lowlands
OD 34 (412.08–419.12 m, 1218–1242 ka); mean pollen sum: 762 (591 excl. Pines)	relatively high sand %, high TIC & TOC (plateau), high and fluctuating $\delta^{18}O$	AP > 93% (mean 97%), *Quercus* dominant (max 44.7%); high AP conc. (mean 80 × 10^3 grains g^{-1}); max mesophilous 59.8% (mean 42.6%), max *Q. cerris* (30.6%), max *Q. robur* (17.1%), max *Carya* (6.3%); max montane 47.7% (mean 31%), max Cedrus (41.1%), max *Abies (*12.4%), max Tsuga (9.9%), max *Betula* (7.3%); max mediterranean 1.1% (mean 0.5%); max riparian 1.9% (mean 0.6%)	closed evergreen (*Cedrus* dominant) and mixed forests in the montane zone, deciduous forests with thermophilous species
OD 35 (419.76–424.56 m, 1243–1264 ka); mean pollen sum: 1729 (385 excl. Pines)	low sand %, low and fluctuating TIC & TOC	AP > 44% (mean 84%), *Pinus sylvestris* dominant (max 91.8%); relative low AP conc. (mean 23 × 10^3 grains g^{-1}); max mesophilous 23.8% (mean 10.9%); max montane 14.7% (mean 6.6%), max *Pinus peuce* (7.6%); max mediterranean 0.4% (mean 0.1%); max riparian 0.3% (mean 0.1%); max Amaranthaceae (28.9%), max *Artemisia* (11.7%), max Poaceae (6.8%)	Pine forests dominant associated with montane tree stands, mesophilous tree stands; extensive open steppe vegetation
OD 36 (424.88–428.08 m, 1265–1291 ka); mean pollen sum: 944 (511 excl. Pines)	relatively high sand %, relatively high and decreasing TIC, high and fluctuating TOC & $\delta^{18}O$ (maxima)	AP > 74% (mean 94%), *Quercus* dominant (max 32%); very high AP conc. (mean 123 × 10^3 grains g^{-1}); max mesophilous 40.3% (mean 25.8%), max *Q. cerris* (16.1%), max *Q. robur* (15.9%), max *Corylus* (5.8%); max montane 35% (mean 23.6%), max *Cedrus* (20.5%), max *Picea abies (17.6%),* max *Abies (*11.1%), max *Fagus* (5.4%); max mediterranean 0.9% (mean 0.3%); max riparian 4.1% (mean 1.3%)	closed evergreen (*Cedrus* dominant) and mixed forests in the montane zone, deciduous forests with thermophilous species, riparian forests
OD 37 (428.72–431.28 m, 1292–1304 ka); mean pollen sum: 941 (452 excl. Pines)	relatively high and fluctuating sand %, low and fluctuating TIC & TOC	AP > 70% (mean 80%), *P. sylvestris* dominant (max 57.7%); relatively low AP conc. (mean 22 × 10^3 grains g^{-1}); max mesophilous 47% (mean 19.6%); max montane 20.7% (mean 10.9%), max *Pinus peuce* (6.5%); max mediterranean 0.3% (mean 0.1%); max riparian 1% (mean 0.7%); max Poaceae (11.8%), max *Artemisia* (6.5%), max Amaranthaceae (5.1%)	Pine forests dominant associated with montane tree stands, mesophilous tree stands; extensive grasslands associated with open steppe vegetation
OD 38 (431.92–436.4 m, 1305–1321 ka); mean pollen sum: 1008 (564 excl. Pines)	relatively high sand %, high TIC (plateau) & TOC, relatively low and fluctuating $\delta^{18}O$	AP > 86% (mean 94%), *Quercus* dominant (max 27.1%); relative high AP conc. (mean 51 × 10^3 grains g^{-1}); max mesophilous 33.9% (mean 25.5%), max *Q. cerris* (18.8%), max *Q. robur* (8.6%); max montane 34.3% (mean 24.8%), max *Abies* (17.6%), max *Cedrus* (14.5%), max *Pinus peuce (10.7%),* max *Fagus* (4.6%); max mediterranean 1.6% (mean 0.8%); max riparian 2.5% (mean 1.4%)	closed evergreen (*Cedrus & Abies* codominant) and mixed forests in the montane zone, deciduous forests with thermophilous species
OD 39 (437.04–439.76 m, 1322–1345 ka); mean pollen sum: 485 (278 excl. Pines)	maximum and fluctuating sand %, low TIC & TOC	AP > 59% (mean 74%), *P. sylvestris* dominant (max 50.1%); low AP conc. (mean 11 × 10^3 grains g^{-1}); max mesophilous 32.5% (mean 16.5%); max montane 19.4% (mean 13.4%), max *P. cembra* (11.9%), max *Cedrus* (5.5%); max mediterranean 1% (mean 0.3%); max riparian 26.1% (mean 3.5%), max *Alnus* (22.1%); max Poaceae (14.6%), max *Artemisia* (9.5%), max Amaranthaceae (9.4%)	Pine forests dominant associated with montane tree stands, mesophilous tree stands; extensive riparian forests and grasslands associated with open steppe vegetation
OD 40 (440.24–447.28 m, 1346–1365 ka); mean pollen sum: 801 (708 excl. Pines)	high and fluctuating sand %, high TIC (plateau), low and increasing TOC, relatively low and fluctuating $\delta^{18}O$	AP > 78% (mean 87%), *Quercus* dominant (max 52.5%); relative high AP conc. (mean 60 × 10^3 grains g^{-1}); max mesophilous 65.2% (mean 54.7%), max *Q. cerris* (39.1%), max *Q. robur* (33.4%), max *Corylus* (12.4%); max montane 23.2% (mean 15.3%), max *Cedrus* (10.1%), max *Tsuga* (7.9%), max *Abies* (7.3%), max *Fagus* (5.1%); max mediterranean 4.4% (mean 1.7%); max riparian 11.3% (mean 4.2%), max *Alnus* (7.3%), max Cyperaceae (14.1%), max Poaceae (8.9%)	closed evergreen and mixed forests in the montane zone, deciduous forests with thermophilous and sclerophyllous species; extensive riparian forests, grasslands and sedgelands

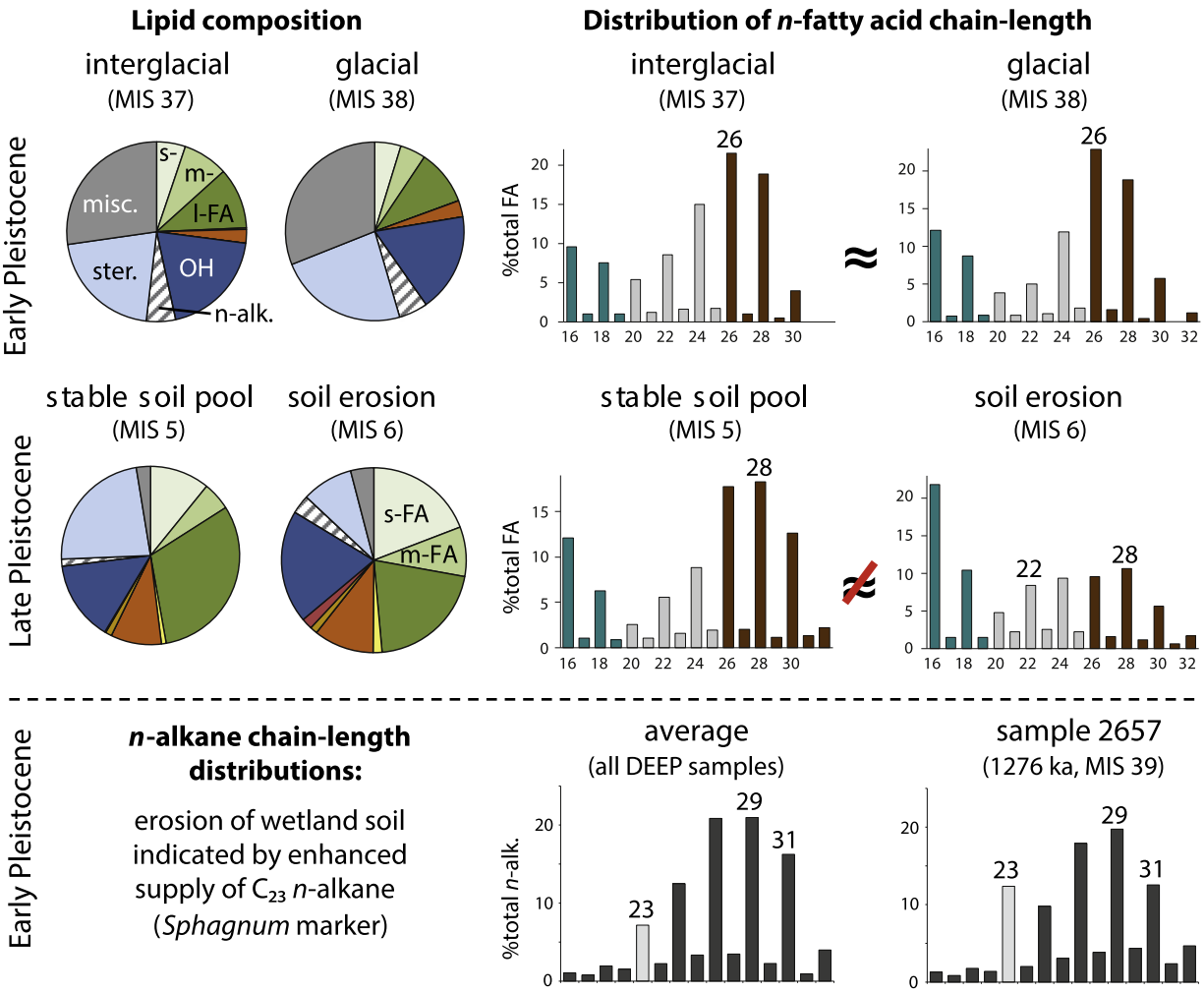

Fig. 6. Comparison of average total lipid composition (pie charts) and *n*-fatty acid distributions (bar diagrams) from glacial (MIS 38, MIS 6) and interglacial (MIS 37, MIS 5) samples from the Early and Late Pleistocene. Chain-length distribution y-axis values are percentages of the total amount of fatty acids; s-, m-, l-FA = short-, mid- and long-chain fatty acids, respectively, ster. = sterols, *n*-alk. = *n*-alkanes, misc. = miscellaneous compounds (mostly diols and hopanoids). Enhanced supply of root-derived compounds (C_{22} and C_{24} *n*-fatty acids from suberin) in samples from Late Pleistocene glacial MIS 6 suggests increased contribution from the soil OM pool (data from Holtvoeth et al., 2017) while the near identical fatty acid distributions dominated by leaf wax-derived long-chain fatty acids imply a stable soil pool in Early Pleistocene climatic cycles (this study). DEEP sample 2657 (1278 ka) showing *Sphagnum* sp. marker peak compared to mean Early Pleistocene *n*-alkane distribution.

Over the last 1365 ka, periods of higher spring and summer temperatures (interglacial intervals) correspond to increased precipitation and preservation of endogenic calcite in the Lake Ohrid DEEP sediments (high TIC content in lithotype 1; Francke et al., 2016; Wagner et al., 2019). High BSi content (average values of 9%) in the sediments of lithotype 1 indicates high numbers of diatom valves in the sediments of Lake Ohrid and/or sponge spicules (Vogel et al., 2010; Francke et al., 2016). During these intervals rather low diol/loliolide ratios suggest higher abundance of diatoms over eustigmatophytes. High eutrophic diatom percentages (max 42%) and green algae (*Pediastrum* and *Botryococcus*) concentrations (max 118×10^3 and 12×10^3 coenobia g^{-1}), especially in the older half of the study interval, suggest a rather productive aquatic environment with high nutrient availability (Fig. 2). These periods of increased aquatic primary productivity are indicative of interglacial conditions and are mostly synchronous with periods of high terrestrial primary productivity (AP/NAP % and concentrations; Fig. 3). By contrast, green algae concentrations from the Late Pleistocene are very low for the last 190 ka indicating a large oligotrophic lake, and green algae concentration maxima of *Pediastrum* and *Botryococcus* for the last 500 ka do not exceed 21×10^3 and 36×10^3 coenobia g^{-1} respectively (unpublished data). In comparison, *Pediastrum* and *Botryococcus* concentration maxima (1265×10^3 and 40×10^3 coenobia g^{-1}) synchronous to TIC and TOC peaks, indicating periods of increased seasonal algae blooms, have been reported during the last 90 ka at Lake Prespa (Panagiotopoulos, 2013).

Sediments characterized by low TIC content (lithotypes 2 and 3) correspond to intervals of reduced aquatic primary productivity and/or poor calcite preservation and are frequently associated with authigenic siderite formed in superficial sediments under rather acidic and reducing conditions during early diagenesis (Francke et al., 2016; Lacey et al., 2016). BSi content is lower on average in these lithotypes (mean 7.5%) suggesting lower diatom abundances, which is in agreement with higher diol/loliolide ratios indicating higher eustigmatophyte populations (Fig. 2). A notable deviation is visible during the first glacial (MIS 42; OD 39), when sustained low diol/loliolide ratios, pointing to increased diatom abundances, occur and are synchronous to the maximum sand content in the study interval (40%; Fig. 2). Low eutrophic diatom percentages and green algae concentrations (*Pediastrum* and *Botryococcus*) occur within intervals with low TIC content (<2%) and indicate lower

primary productivity. These intervals are associated with glacial and transitional conditions and are further characterized by reduced terrestrial productivity (AP/NAP % and concentrations) suggesting a drier and colder climate, reduced runoff and lower nutrient availability.

The occurrence of bivalve shell fragments between 1364 ka and 1293 ka suggests that the coring site was situated within the natural habitat of bivalves and/or they were transferred to the DEEP site by waves and currents. Bivalve shell fragments are encountered in Lake Ohrid DEEP sediments below 447 mcd (older than 1365 ka) and are confined to the first 70 ka since the onset of continuous lacustrine sedimentation at 1365 ka. A conspicuous *Dreissena* shell horizon synchronous with low deciduous tree percentages, high green algae concentrations and a pronounced Poaceae peak, which could indicate high *Phragmites* abundance, has been reported from Lake Prespa during the last glacial (Panagiotopoulos et al., 2014): The authors interpreted this event as a drop in lake level associated with the expansion of littoral zone habitats that triggered mussel population and reed bed growth. *Dreissena* populations typically occur in the upper sub-littoral zone (10–35 m water depth) in modern Lake Ohrid ecosystems (Albrecht and Wilke, 2008; Cvetkoska et al., 2018; Wilke et al., 2010). Consequently, the absence of shell fragments in the younger half of the study interval indicates increasing water depth.

Several lake proxies apparently capture this gradual expansion of the lake over the first 100 kyr of its continuous existence (1365–1265 ka; Fig. 2). Green algae, aquatic vascular plant, and Poaceae show higher abundances over this interval encompassing this first phase of lake development. *Pediastrum* and *Botryococcus* reach their maximum values within this interval and indicate eutrophic waters and extensive submerged and littoral vegetation (Jankovská and Komárek, 2000). Considering the concomitant high grass (including *Phragmites*) and aquatic vascular plant (including emergent, submerged and floating species; Section 3.3) percentages and concentrations, extensive wetlands most likely surrounded the lake during these first phases. There is a clear dominance of littoral diatom species (0–10 m) over the older half of the study period, with some of the most prominent peaks within glacial intervals. Some of these peaks (e.g. in MIS 42 and MIS 40) also occur in grass and aquatic vascular plant percentages and can most likely be attributed to lake level drops. Pine percentages appear to diverge from the typical glacial maxima-interglacial minima pattern, which occur in the younger half of the study interval. Pine pollen grain's morphology allows for their excellent dispersal and are found to be commonly overrepresented in large water bodies (e.g. Sadori et al., 2016). We postulate that the gradual increase in pine pollen percentages over the initial lake development stages most likely conveys the long-term increase of the lake surface area.

A transition to higher $\delta^{18}O_c$ over the first 100 kyr of the study interval suggests a progression from fresher to more evaporative conditions (Fig. 2; Lacey et al., 2016), which is most likely a function of increasing surface area and a longer water residence time associated with an expansion of lake volume. Variations in $\delta^{13}C_c$ are decoupled from the overall trend to higher $\delta^{18}O_c$ (Fig. 3), indicating the lake was hydrologically open and that the $\delta^{18}O_c$ baseline shift was probably driven by lake ontogenetic processes rather than a climate forcing mechanism. In the shallower lake environment at the start of the study interval, variations in aquatic productivity may exert a stronger control on $\delta^{13}C_c$ via the preferential removal of ^{12}C during interglacial periods characterized by higher temperatures and nutrient availability. Lower temperatures during glacial periods would reduce rates of productivity and so drive lower $\delta^{13}C_c$, which is observed particularly during the inception and termination of MIS 42 (Fig. 3). This relationship is in contrast with that of the deeper lake setting of the upper record that buffers productivity-related control on $\delta^{13}C_c$, and instead is primarily a function of hydrology, karst throughflow activity, and catchment soil development (Lacey et al., 2016).

High BIT index values (above 0.85) over the entire study interval reflect higher contribution of branched GDGTs (brGDGTs) over isoprenoid GDGTs (iGDGTs). By contrast, iGDGTs dominate in Late Pleistocene sediments, indicating significantly higher production of biomass by Thaumarchaeota (BIT below 0.3; Holtvoeth et al., 2017). Thaumarchaeota have been found to thrive in low-nutrient settings (Könneke et al., 2014). The fact that iGDGTs are nearly absent in the Early Pleistocene sediments, especially during interglacials, would therefore support the assumption of a high-nutrient aquatic environment that either suppresses or dilutes biomass production from Thaumarchaeota. However, a successively increasing contribution of iGDGTs during glacial intervals is clearly recognizable as time progresses, which indicates increasingly nutrient-depleted conditions during times of low terrestrial run-off. Such conditions may result from successively less efficient uptake of nutrients recycled back into the water column from the sediment as the water depth increases, with stratification becoming more frequent and the sediment surface eventually lying below the photic zone. Thus, the observed trend of minima in the BIT record becoming more pronounced reflects the early stages of Lake Ohrid ultimately developing towards a deep and oligotrophic ecosystem.

Most of the trends from independent lines of evidence presented above suggest that the Lake Ohrid system crossed a threshold approximately in the middle of the study interval around 1265 ka (within MIS 39; OD 36). Close inspection of the TIC content shows a rather atypical interglacial seesaw shape in contrast to the typical plateau also seen in AP % and BIT (Fig. 2). Prominent peaks at 1277 ka in TOC, AP, pine, montane, mesophilous and microscopic charcoal concentrations suggest that the drop in TIC is driven by increased input of carbonate-free material rather than climate induced. Indeed, very high TIC content (>8.5%), very low Ti/K, and high AP over the older half of the record and MIS 43 (OD 40), in particular, point to a restricted supply of terrestrial material and enhanced soil development under a dense tree canopy. Low Ti/K is indicative for increased supply of dissolved K, secondary clay minerals and thus for improved soil development in the catchment of Lake Ohrid (Francke et al., 2019). A distinct trend towards higher $\delta^{18}O_c$ during MIS 39 (up to +3‰; Fig. 5) also supports the existence of a transitional phase in lake ontogeny during this interval, implying that the hydrology of Lake Ohrid underwent a fundamental change to a new base state characterized by a permanent deep-water body that has persisted to present day.

Most likely the extended wetlands surrounding the lake during the initial phases of the lake development served as a trap accumulating the bulk of the eroded material delivered by surface runoff. This temporarily stored alluvial material probably contributes to the siliciclastic material that dilutes the carbonate/TIC during MIS 39 when it is resuspended/eroded as the lake expands and drowns the surrounding wetlands. Combined uranium isotope and palynological data from the DEEP core during the Late Glacial and Holocene suggest that increasing vegetation cover in peak interglacial conditions restrict erosion of thinner soils at higher altitudes (Francke et al., 2019). Enhanced supply of the C_{23} *n*-alkane (Fig. 6) deriving from peat moss (*Sphagnum* sp. typically encountered in wetlands; see also Section 4.4) registered at 1277 ka attests to the erosion of surrounding wetland soil, followed by erosion of the underlying siliciclastics.

During the study interval, Lake Ohrid underwent a gradual expansion in lake size and depth as observed in the lithology, abiotic and biotic lake proxies (Fig. 2). This was not a linear process and most likely included a series of expansion events coupled with

shifts in climate and catchment dynamics. The gradual deepening of the lake and the increasing distance of the DEEP site from the lake shore seem to be in agreement with lake proxy data attaining values closer to those characterizing later phases of lake development over the Pleistocene upcore (e.g. absence of shell fragments, increase of planktonic diatoms, $\delta^{18}O_c$ and $\delta^{13}C_c$, and a parallel decline of aquatic vascular plants, green algae, grasslands). The mechanisms driving these long-term changes in the Lake Ohrid hydrology are most likely a combination of local (tectonic subsidence) and global (higher amplitude climate cycles) factors.

5.2. Early Pleistocene plant diversity and vegetation dynamics

Early Pleistocene pollen spectra from the Lake Ohrid DEEP site reveal a diverse palynoflora with a total of 65 tree, shrub and vine taxa and 53 upland herbs. Relict tree species such as *Cedrus, Tsuga, Carya, Pterocarya, Cathaya, Liquidambar* and *Parrotia* formed important constituents of the Early Pleistocene flora of the Ohrid catchment (e.g. *Cedrus* and *Tsuga* up to 41% and 17% respectively; Fig. 5). These Arcto-Tertiary Geoflora elements had a much wider past distribution occurring across the northern hemisphere during the Neogene (e.g González-Sampériz et al., 2010; Magri et al., 2017; Postigo-Mijarra et al., 2010; Tallis, 1991), but eventually became extinct regionally over the Pleistocene (Sadori et al., 2016; Kousis et al., 2018; Sinopoli et al., 2018). Pollen percentages of these Neogene 'relict' tree species indicate continuous presence in the catchment during interglacials, which are characterized by a remarkable diversity (selected pollen taxa with abundance greater than 2% are shown in Fig. 4). These findings are in agreement with pollen records from southern Italy (see reviews by Bertini, 2010; Combourieu-Nebout et al., 2015) and point to the refugial characteristics of the Italian and Balkan peninsulas. Thermophilous trees found in modern European flora survived preceding glacials in southern Mediterranean refugia such as the intramontane basins in southern Europe (e.g. Tzedakis et al., 2002; Panagiotopoulos et al., 2014; Combourieu-Nebout et al., 2015; Sadori et al., 2016). When a relict species no longer finds suitable habitats to grow within these refugia, its population will diminish at the continental scale and eventually disappear (e.g. Bennett et al., 1991). Indeed, palynological analyses at 64-cm-resolution of the last 0.5Ma of the Ohrid DEEP core (Sadori et al., 2016), and 16-cm-resolution of the MIS 11 (Kousis et al., 2018) and MIS 5 (Sinopoli et al., 2018) suggest receding populations of these trees throughout the EMPT and the last extinction events occurring gradually within high-amplitude climatic cycles of the Middle Pleistocene.

Arboreal percentages and concentrations (AP/NAP) imply a rather forested landscape within the Ohrid catchment throughout the study interval (Table 1; Fig. 3). Phases of increased landscape openness are usually characterized by higher palynological richness, allowing for a better representation of herbaceous species (Birks and Line, 1992; see also Section 3.3). Despite the presence of extended open-landscape areas with increasing altitude, palynological richness in Late Pleistocene samples from neighboring Lake Prespa (849 m asl; Panagiotopoulos, 2013) is substantially lower than Early Pleistocene samples from Lake Ohrid (693 m asl; Fig. 5). Graminoid with forb dominated biomes (GRAM) were reconstructed for five samples only and occurred within glacial intervals (three of them within OD 35, MIS 38), when *Artemisia* and Amaranthaceae reach their maximum percentages. Subsequently, minima in palynological richness, $E(T_{400})$, occur in OD 35 samples with high arboreal percentages (maximum *P. sylvestris*-type abundance) and are most likely related to the flooding of grasslands and wet meadows characterized by high herbaceous species diversity (Figs. 4 and 5). Abrupt vegetation turnovers during MIS 38 have been also reported from a high-resolution marine record off the Portuguese margin and concomitant excursions in planktonic $\delta^{18}O$ (maxima in *Artemisia*, Amaranthaceae, Poaceae match peaks in planktonic oxygen isotopes) were attributed to North Atlantic millennial-scale type variability (Tzedakis et al., 2015). However, these exceptionally high Amaranthaceae percentages (up to 27%) could also be traced back to significant lake-level shifts occurring while the lake system entered a new equilibrium state (Section 5.1). There is no evidence for root-derived material, apart from two samples in OD 32 (MIS 35), suggesting that the soil organic matter pool was permanently stabilized by a closed vegetation cover that was not affected by hydrological changes to the same extent as observed during Late Pleistocene climate oscillations (Fig. 6; Holtvoeth et al., 2017). The parallel occurrence of conifer and deciduous forests within the Ohrid catchment suggests the availability of suitable habitats where these distinct plant communities were dominant. Decreasing Poaceae (including grasses and macrophytes) and Cyperaceae percentages upcore are most likely linked to the inundation of wetlands and lowland areas surrounding the lake. At this point, it should be noted that during the first stages of the Lake Ohrid development (Section 5.1) the pollen record may reflect shifts occurring at a more local scale in comparison to a more regional signal captured in the second half.

For instance, the montane group abundance remains relatively unchanged over the first climate cycle (MIS 43–42; OD 40–39), whereas mesophilous species, which dominate in lower altitude vegetation zones, experience a significant retraction. Within OD 40 (MIS 43), maximum TIC, MAAT and extremely low Ti/K and values indicate a limited contribution of both siliciclastic material from the catchment and of organic matter from cooler high-altitude areas. During this interval, extensive lowland areas as well as exposed wetland areas bordering the lake appear to have acted as a sediment trap (see also Section 5.1) and limited organic matter input from cooler (and shaded) higher altitude soils, resulting in the maximum GDGT-based reconstructed mean annual air temperature values (Fig. 3). As the lake expanded and lowland areas became submerged, organic matter input from forested (shaded) areas within the catchment increased and may thus have caused the MAAT values to drop significantly. As in-lake production of brGDGTs cannot be ruled out an additional or alternative mechanism for decreasing MAAT values may be an increasing proportion of brGDGTs produced in increasingly deeper and cooler parts of the water column. In both cases, however, the generally decreasing trend of the first 80–100 ka in MAAT reflects changes catchment configuration and/or lake morphometry rather than an underlying actual cooling of the local climate.

The most frequently reconstructed biome during interglacial periods is cool mixed evergreen needleleaf and deciduous broadleaf forests (CMIX) that probably reflects a well-developed montane belt above the oak-dominated zone, whereas cool evergreen needleleaf forests (COOL) dominated by *Pinus sylvestris*-type prevail during glacials (Fig. 4). Montane and mesophilous abundances rise rapidly after each deglaciation. The primary succession of tree species within the five interglacial periods examined provides unique insights into the 41-kyr world. The succession begins with an early expansion of deciduous forests (*Quercus* accompanied by other mesophilous and thermophilous trees e.g. *Carya, Carpinus betulus, Ulmus,* and *Zelkova*), followed by an increase of montane forests (first *Abies* associated with *Fagus,* followed by *Cedrus, Tsuga* and *Betula*). A final transitional phase characterized by an increase of *Quercus* or *Picea* can be observed in the younger half of the record. Glacial pollen spectra are dominated by pines and herbaceous vegetation (mostly Poaceae, Amaranthaceae, Cichorioideae, and *Artemisia*) with low but continuous percentages of mesophilous and montane species suggesting the occurrence of an open woodland within the Ohrid catchment. Mediterranean

sclerophyllous plant abundances (dominated by evergreen oaks) are quite low and the maximum values are recorded at 1356 ka shortly after the most prominent June insolation peak within the study interval (max 4.4% in OD 43 mainly by *Quercus ilex*-type 2.9%; Figs. 3 and 4).

The succession pattern emerging from the Early Pleistocene Ohrid record bears similarities with the regionally adapted scheme of idealized vegetation phases (pre-temperate phase of open woodland; temperate phase of Mediterranean, deciduous and montane forests; post temperate phase of open woodland and steppe vegetation during glacials) for southern European refugia for the Late Pleistocene (Tzedakis, 2007 and references therein). Mediterranean paleobotanical records from the Late Pliocene and Early Pleistocene are usually fragmented and their age assignment is often ambiguous. Considering chronological uncertainties, Lake Ohrid pollen spectra are floristically closer to pollen sequences from southern Italy and in particular the Crotone Basin (e.g. Combourieu-Nebout, 1993; Joannin et al., 2007; Suc et al., 2010). The Early Pleistocene Semaforo-Vrica sequences with an estimated age between 2.47 and 1.34 Ma record an increase of deciduous forests (*Quercus*), followed by subtropical humid forests ("Taxodiaceae" and *Cathaya*), succeeded by altitudinal coniferous forests (*Tsuga, Cedrus, Abies,* and *Picea*) during interglacials and an open vegetation phase (Poaceae, Cichorioideae, Asteroideae, and *Artemisia*) during glacials (Combourieu-Nebout, 1993). The neighboring Santa Lucia sequence with an estimated Early Pleistocene age (1360–1280 ka; Joannin et al., 2007) shows a closer affinity to the Ohrid palynoflora (limited "Taxodiaceae" and *Cathaya* contribution) and the authors propose a three-phased succession of deciduous forests (warm), coniferous forests (cool and humid), and open woodland (cold and dry).

One of the most striking features of the Lake Ohrid pollen record is the extraordinary diversity and abundance of Neogene relict tree species in the composition of the regional Early Pleistocene (palyno)flora. Palynological richness remains high throughout the study interval with distinct maxima occurring in OD 40 and 39 and minima in OD 35. Total relict percentages attain values of up to 48% (OD 34; MIS 37; Fig. 5) within interglacials that is exceptional compared to other regional palynofloras of the same age (e.g. Magri et al., 2017). Considering that pines are not excluded from the pollen sum (Section 3.2), these values suggest that relict tree taxa such as *Cedrus*, *Tsuga*, *Carya*, and *Pterocarya* comprised integral species of the vegetational succession cycles summarized above. Continuous presence and high abundances (several species above 5%) of relict species confirm that the Ohrid region served as a Mediterranean tree refugium throughout the last 0.5Ma (see also Sadori et al., 2016). The ecological succession of forest species appears to be distinct for each glacial-interglacial cycle. For instance, montane forests of *Abies* associated with *Fagus* are the dominant climax vegetation in the older half of the record, whereas *Tsuga* associated with *Betula* climax communities characterize the younger half (Fig. 4). Distinct patterns of ecological succession are commonly the outcome of different abiotic and biotic processes influencing forest species composition and succession such as changes in climate, soil nutrient availability, interspecific competition, and frequency of disturbance events (e.g. wildfires). In fact, a period of increased microscopic charred particle concentrations occurring after a June insolation peak within OD 36 (MIS 39), points to an increase of fire frequency and might have contributed to a reorganization of the vegetation within the Ohrid catchment.

By comparison, relict species recorded in the Tenaghi Philippon pollen archive from northwestern Greece during the Early Pleistocene show rather limited abundance (Van Der Wiel and Wijmstra, 1987; Tzedakis et al., 2006). In this almost continuous peat sequence (two short hiatuses of 2 and 1.3 m are reported for the lower part; van der Wiel and Wijmstra, 1987), relict species percentages are confined below 5% with the exception of a *Tsuga* peak of ~9% at 1315 ka (after the new age model of Tzedakis et al. (2006). These differences in relict species abundance between the Lake Ohrid and Tenaghi Philippon archives can be attributed to contrasting location (e.g. relict tree populations occurring *in situ* vs. in the vicinity of the basin), altitude (mid vs. low), and depositional environment traits (lake vs peat/wetland). Despite these differences, relict species occurrences and extinctions reported from these two well-dated long pollen records provide insights into bioclimatic gradients and past species distribution back to the Early Pleistocene.

As it has been proposed for the Late Pleistocene (e.g. Tzedakis et al., 2002; Panagiotopoulos et al., 2014; Sadori et al., 2016), mid-altitude sites in the western part of the Balkan peninsula appear to have experienced a less pronounced seasonal water stress during the Early Pleistocene (e.g. low sclerophyllous plant abundances point to limited summer drought) and over glacial intervals (e.g. rather limited steppe vegetation elements suggest an open woodland landscape). Moreover, a high abundance of montane relict species (e.g. *Cedrus* and *Tsuga*) emphasizes the importance of these mid-altitude sites, which are characterized by sufficient moisture availability even during glacial intervals, for the survival of these species during ensuing high-amplitude climate oscillations over the course of the Pleistocene. Further studies based on quantitative climate reconstructions are needed to constrain the amplitude and nature of climate variability during the Early Pleistocene in the region.

6. Conclusions

Here we present a unique pollen archive from a southern European mid-altitude refugium registering vegetation dynamics in the obliquity-paced world. Based on a robust chronology, the Lake Ohrid sequence spans continuously the last 1.36 Ma. The study interval comprises the first 200 kyr of lake development (1365–1165 ka; MIS 43–35), when the lake was relatively shallow and sustained generally higher nutrient levels compared to the Late Pleistocene, although there is evidence for increasing nutrient depletion during glacial stages. Palynological data are complemented with biomarker, diatom, geochemical and sedimentological data to better constrain shifts in the depositional environment.

A gradual expansion in lake size and depth can be traced in several aquatic abiotic and biotic proxies. Within the first 100 ka years of its existence, Lake Ohrid experienced a series of expansion events coupled with shifts in climate and catchment dynamics. Aquatic vascular plants, algae, organic and inorganic geochemistry, and sedimentology indicate that periods of low lake-levels and high nutrient load occurred less frequently upcore. A gradual increase in water depth and distance from shore are inferred for the DEEP coring site during the study interval. This process was not linear, rather, independent lines of evidence suggest that the lake system crossed a critical threshold at approximately 1265 ka (MIS 39) and subsequently entered a new equilibrium state (within the period examined). The timing of this major shift to a deeper and larger lake system coincides broadly with the onset of the Mid-Pleistocene climate transition. Hence, local drivers of environmental change, such as ongoing basin subsidence, most likely played an equally important role to climate in establishing a new equilibrium state for the young Lake Ohrid (eco)system.

Obliquity-paced climatic cycles drive changes in vegetation cover within the Ohrid catchment (mean PASZ duration of ~21 ka), although precession-driven insolation shifts appear to control mesophilous species response during interglacials (distinct M-

shaped peaks tracing June insolation double peaks in MIS 37 and 35). Pollen and biomarker data indicate forested and productive terrestrial ecosystems prevailing during interglacials and a rather open woodland landscape with a still relatively stable soil pool during glacials, which is most likely due to the shorter duration and lower amplitude characterizing Early Pleistocene climatic cycles. The most frequently reconstructed biome during interglacial periods is cool mixed evergreen needleleaf and deciduous broadleaf forests, while cool evergreen needleleaf forests dominate within glacials. The vegetation succession pattern and the extraordinary relict tree diversity and abundance (comprising up to half of the total arboreal vegetation) emerging from Early Pleistocene pollen spectra confirm the hypothesis that the Ohrid basin has been an important Quaternary refugium in the Mediterranean region. Continuous presence of several mesophilous and montane (including relicts) species over successive climatic cycles indicate sufficient moisture availability allowing an assemblage of plants with distinct climatic tolerances and habitat preferences to grow in the Ohrid region throughout the study interval. Low values of Mediterranean sclerophyllous species imply winter temperatures similar to modern day and the absence of periods characterized by extended seasonal (summer) drought.

Acknowledgements

The SCOPSCO Lake Ohrid drilling campaign was funded by the ICDP, the German Ministry of Higher Education and Research, the German Research Foundation, the University of Cologne (Germany), the British Geological Survey (United Kingdom), the INGV and CNR (Italy), and the governments of the republics of North Macedonia and Albania. Logistic support was provided by the Hydrobiological Institute in Ohrid. Drilling was carried out by Drilling, Observation and Sampling of the Earth's Continental Crust (DOSECC) and using the Deep Lake Drilling System (DLDS). We thank K. Schittek for insightful comments on previous manuscript versions, and N. Mantke and D. Klinghardt for lab work coordination. Palynological processing was performed with the assistance of K. Knoedgen, S. Kyrikou, N. Mai, and L. Swawatzki. K. Panagiotopoulos acknowledges funding from the German Research Foundation (DFG grant PA 2664/2-1). We would like to thank two anonymous reviewers for their comments that helped improve this manuscript.

References

Albrecht, C., Wilke, T., 2008. Ancient Lake Ohrid: biodiversity and evolution. Hydrobiologia 615 (1), 103–140.

Altolaguirre, Y., Postigo-Mijarra, J.M., Barrón, E., Carrión, J.S., Leroy, S.A.G., Bruch, A.A., 2019. An environmental scenario for the earliest hominins in the Iberian Peninsula: early Pleistocene palaeovegetation and palaeoclimate. Rev. Palaeobot. Palynol. 260, 51–64.

Bennett, K.D., 2008. PSIMPOLL and PSCOMB (Version 4.26) Programs for Plotting and Analysis last access: 05.07.2019, available at: http://chrono.qub.ac.uk/psimpoll/psimpoll.html.

Bennett, K.D., Tzedakis, P.C., Willis, K.J., 1991. Quaternary refugia of north European trees. J. Biogeogr. 18 (1), 103–115.

Bertini, A., 2001. Pliocene climatic cycles and altitudinal forest development from 2.7 Ma in the northern Apennines (Italy): evidence from the pollen record of the Stirone section (~ 5.1 t0 ~ 2.2 Ma). Geobios 34 (3), 253–265.

Bertini, A., 2010. Pliocene to Pleistocene palynoflora and vegetation in Italy: state of the art. Quat. Int. 225 (1), 5–24.

Beug, H.J., 2004. Leitfaden der Pollenbestimmung für Mitteleuropa und angrenzende Gebiete, München, p. 542.

Bhagwat, S.A., Willis, K.J., 2008. Species persistence in northerly glacial refugia of Europe: a matter of chance or biogeographical traits? J. Biogeogr. 35 (3), 464–482.

Birks, H.J.B., Line, J.M., 1992. The use of rarefaction analysis for estimating palynological richness from Quaternary pollen-analytical data. Holocene 2 (1), 1–10.

Bush, R.T., Mcinerney, F.A., 2013. Leaf wax n-alkane distributions in and across modern plants: implications for paleoecology and chemotaxonomy. Geochem. Cosmochim. Acta 117, 161–179.

Clark, P.U., Archer, D., Pollard, D., Blum, J.D., Rial, J.A., Brovkin, V., Mix, A.C., Pisias, N.G., Roy, M., 2006. The middle Pleistocene transition: characteristics, mechanisms, and implications for long-term changes in atmospheric pCO2. Quat. Sci. Rev. 25 (23–24), 3150–3184.

Combourieu-Nebout, N., 1993. Vegetation response to upper Pliocene glacial/interglacial cyclicity in the central mediterranean. Quat. Res. (Orlando) 40 (2), 228–236.

Combourieu-Nebout, N., Bertini, A., Russo-Ermolli, E., Peyron, O., Klotz, S., Montade, V., Fauquette, S., Allen, J., Fusco, F., Goring, S., Huntley, B., Joannin, S., Lebreton, V., Magri, D., Martinetto, E., Orain, R., Sadori, L., 2015. Climate changes in the central Mediterranean and Italian vegetation dynamics since the Pliocene. Rev. Palaeobot. Palynol. 218, 127–147.

Combourieu-Nebout, N., Grazzini, C.V., 1991. Late Pliocene northern hemisphere glaciations: the continental and marine responses in the central Mediterranean. Quat. Sci. Rev. 10 (4), 319–334.

Cvetkoska, A., Levkov, Z., Reed, J.M., Wagner, B., 2014. Late Glacial to Holocene climate change and human impact in the Mediterranean: the last ca. 17ka diatom record of Lake Prespa (Macedonia/Albania/Greece). Palaeogeogr. Palaeoclimatol. Palaeoecol. 406, 22–32.

Cvetkoska, A., Pavlov, A., Jovanovska, E., Tofilovska, S., Blanco, S., Ector, L., Wagner-Cremer, F., Levkov, Z., 2018. Spatial patterns of diatom diversity and community structure in ancient Lake Ohrid. Hydrobiologia 819 (1), 197–215.

De Beaulieu, J.-L., Andrieu-Ponel, V., Reille, M., Grüger, E., Tzedakis, C., Svobodova, H., 2001. An attempt at correlation between the Velay pollen sequence and the Middle Pleistocene stratigraphy from central Europe. Quat. Sci. Rev. 20 (16–17), 1593–1602.

De Jonge, C., Hopmans, E.C., Zell, C.I., Kim, J.-H., Schouten, S., Sinninghe Damsté, J.S., 2014. Occurrence and abundance of 6-methyl branched glycerol dialkyl glycerol tetraethers in soils: implications for palaeoclimate reconstruction. Geochem. Cosmochim. Acta 141, 97–112.

Fletcher, W.J., Sánchez Goñi, M.F., Allen, J.R.M., Cheddadi, R., Coumbourieu-Nebout, N., Huntley, B., Lawson, I.T., Londeix, L., Magri, D., Margari, V., Müller, U.C., Naughton, F., Novenko, E., Roucoux, K.H., Tzedakis, P.C., 2010. Millennial-scale variability during the last glacial in vegetation records from Europe. Quat. Sci. Rev. 29, 2839–2864.

Follieri, M., Magri, D., Sadori, L., 1989. Pollen stratigraphical synthesis from valle di Castiglione (roma). Quat. Int. 3, 81–84.

Francke, A., Dosseto, A., Panagiotopoulos, K., Leicher, N., Lacey, J.H., Kyrikou, S., Wagner, B., Zanchetta, G., Kouli, K., Leng, M.J., 2019. Sediment residence time reveals Holocene shift from climatic to vegetation control on catchment erosion in the Balkans, Global Planet. Change 177, 186–200.

Francke, A., Wagner, B., Just, J., Leicher, N., Gromig, R., Baumgarten, H., Vogel, H., Lacey, J.H., Sadori, L., Wonik, T., Leng, M.J., Zanchetta, G., Sulpizio, R., Giaccio, B., 2016. Sedimentological processes and environmental variability at Lake Ohrid (Macedonia, Albania) between 637 ka and the present. Biogeosciences 13 (4), 1179–1196.

Fusco, F., 2010. Picea+Tsuga pollen record as a mirror of oxygen isotope signal? An insight into the Italian long pollen series from Pliocene to Early Pleistocene. Quat. Int. 225 (1), 58–74.

González-Sampériz, P., Leroy, S.A.G., Carrión, J.S., Fernández, S., García-Antón, M., Gil-García, M.J., Uzquiano, P., Valero-Garcés, B., Figueiral, I., 2010. Steppes, savannahs, forests and phytodiversity reservoirs during the Pleistocene in the Iberian Peninsula. Rev. Palaeobot. Palynol. 162 (3), 427–457.

Grimm, E.C., 1992. TILIA and TILIA-graph: pollen spreadsheet and graphics programs. Programs and Abstracts. In: 8th International Palynological Congress, Aix-en-Provence, France, p. 56.

Head, M.J., Gibbard, P.L., 2015. Early–Middle Pleistocene transitions: linking terrestrial and marine realms. Quat. Int. 389, 7–46.

Hoffmann, N., Reicherter, K., Fernández-Steeger, T., Grützner, C., 2010. Evolution of ancient Lake Ohrid: a tectonic perspective. Biogeosciences 7 (10), 3377–3386.

Holtvoeth, J., Vogel, H., Valsecchi, V., Lindhorst, K., Schouten, S., Wagner, B., Wolff A., G., et al., 2017. Linear and non-linear responses of vegetation and soils to glacial-interglacial climate change in a Mediterranean refuge. Sci. Rep. 7 (1), 8121.

Hopmans, E.C., Weijers, J.W.H., Schefuß, E., Herfort, L., Sinninghe Damsté, J.S., Schouten, S., 2004. A novel proxy for terrestrial organic matter in sediments based on branched and isoprenoid tetraether lipids. Earth Planet. Sci. Lett. 224 (1–2), 107–116.

Hughes, P.D., Woodward, J.C., Gibbard, P.L., 2006. Quaternary glacial history of the Mediterranean mountains. Prog. Phys. Geogr. 30 (3), 334–364.

Jankovská, V., Komárek, J., 2000. Indicative value of *Pediastrum* and other coccal green algae in paleoecology. Folia Geobot. 35 (1), 59–82.

Joannin, S., Ciaranfi, N., Stefanelli, S., 2008. Vegetation changes during the late early Pleistocene at Montalbano Jonico (province of Matera, southern Italy) based on pollen analysis. Palaeogeogr. Palaeoclimatol. Palaeoecol. 270 (1–2), 92–101.

Joannin, S., Quillévéré, F., Suc, J.-P., Lécuyer, C., Martineau, F., 2007. Early Pleistocene climate changes in the central Mediterranean region as inferred from integrated pollen and planktonic foraminiferal stable isotope analyses. Quat. Res. (Orlando) 67 (2), 264–274.

Jovanovska, E., Cvetkoska, A., Hauffe, T., Levkov, Z., Wagner, B., Sulpizio, R., Francke, A., Albrecht, C., Wilke, T., 2016. Differential resilience of ancient sister lakes Ohrid and Prespa to environmental disturbances during the Late Pleistocene. Biogeosciences 13 (4), 1149–1161.

Just, J., Nowaczyk, N.R., Sagnotti, L., Francke, A., Vogel, H., Lacey, J.H., Wagner, B., 2016. Environmental control on the occurrence of high-coercivity magnetic minerals and formation of iron sulfides in a 640 ka sediment sequence from

Lake Ohrid (Balkans). Biogeosciences 13 (7), 2093–2109.
Just, J., Sagnotti, L., Nowaczyk, N.R., Francke, A., Wagner, B., 2019. Recordings of fast paleomagnetic reversals in a 1.2 Ma greigite rich sediment archive from Lake Ohrid, Balkans. J. Geophys. Res.
Klok, J., Baas, M., Cox, H.C., De Leeuw, J.W., Rijpstra, W.I.C., Schenck, P.A., 1984. Qualitative and quantitative characterization of the total organic matter in a recent marine sediment (Part II). Org. Geochem. 6, 265–278.
Komárek, J., Jankovská, V., 2001. Review of the Green Algal Genus *Pediastrum*; Implication for Pollen-Analytical Research, vol. 108. Bibliotheca Phycologica, Berlin; Stuttgart, p. 127.
Könneke, M., Schubert, D.M., Brown, P.C., Hugler, M., Standfest, S., Schwander, T., Schada Von Borzyskowski, L., Erb, T.J., Stahl, D.A., Berg, I.A., 2014. Ammonia-oxidizing archaea use the most energy-efficient aerobic pathway for CO2 fixation. Proc. Natl. Acad. Sci. 111 (22), 8239–8244.
Kousis, I., Koutsodendris, A., Peyron, O., Leicher, N., Francke, A., Wagner, B., Giaccio, B., Knipping, M., Pross, J., 2018. Centennial-scale vegetation dynamics and climate variability in SE Europe during Marine Isotope Stage 11 based on a pollen record from Lake Ohrid. Quat. Sci. Rev. 190, 20–38.
Koutsodendris, A., Kousis, I., Peyron, O., Wagner, B., Pross, J., et al., 2019. The Marine Isotope Stage 12 pollen record from Lake Ohrid (SE Europe): Investigating short-term climate change under extreme glacial conditions. Quat. Sci. Rev. 221.
Lacey, J.H., Leng, M.J., Francke, A., Sloane, H.J., Milodowski, A., Vogel, H., Baumgarten, H., Zanchetta, G., Wagner, B., 2016. Northern mediterranean climate since the middle Pleistocene: a 637 ka stable isotope record from Lake Ohrid (Albania/Macedonia). Biogeosciences 13 (6), 1801–1820.
Laskar, J., Robutel, P., Joutel, F., Gastineau, M., Correia, A.C.M., Levrard, B., 2004. A long-term numerical solution for the insolation quantities of the Earth. Astron. Astrophys. 428 (1), 261–285.
Leroy, S.A.G., 1997. Climatic and non-climatic lake-level changes inferred from a Plio-Pleistocene lacustrine complex of Catalonia (Spain): palynology of the Tres Pins sequences. J. Paleolimnol. 17 (4), 347–367.
Leroy, S.A.G., 2007. Progress in palynology of the Gelasian–Calabrian stages in Europe: ten messages. Rev. Micropaleontol. 50 (4), 293–308.
Leroy, S.A.G., 2008. Vegetation cycles in a disturbed sequence around the Cobb-Mountain subchron in Catalonia (Spain). J. Paleolimnol. 40 (3), 851–868.
Levkov, Z., Blanco, S., Krstic, S., Nakov, T., Ector, L., 2007. Ecology of benthic diatoms from Lake macro Prespa (Macedonia). Arch. Hydrobiol. Suppl. Algol. Stud. 124 (1), 71–83.
Lindhorst, K., Krastel, S., Reicherter, K., Stipp, M., Wagner, B., Schwenk, T., et al., 2015. Sedimentary and tectonic evolution of Lake Ohrid (Macedonia/Albania). Basin Res. 27 (1), 84–101.
Lisiecki, L.E., Raymo, M.E., 2005. A Pliocene-Pleistocene stack of 57 globally distributed benthic δ18O records. Paleoceanography 20 (1).
Liu, Y., Basinger, J.F., 2000. Fossil Cathaya (Pinaceae) pollen from the Canadian high arctic. Int. J. Plant Sci. 161 (5), 829–847.
Magri, D., Di Rita, F., Aranbarri, J., Fletcher, W., González-Sampériz, P., 2017. Quaternary disappearance of tree taxa from Southern Europe: timing and trends. Quat. Sci. Rev. 163, 23–55.
Magri, D., Palombo, M.R., 2013. Early to middle Pleistocene dynamics of plant and mammal communities in south west Europe. Quat. Int. 288, 63–72.
Marinova, E., Harrison, S.P., Bragg, F., Connor, S., De Laet, V., Leroy, S.A.G., Mudie, P., Atanassova, J., Bozilova, E., Caner, H., Cordova, C., Djamali, M., Filipova-Marinova, M., Gerasimenko, N., Jahns, S., Kouli, K., Kotthoff, U., Kvavadze, E., Lazarova, M., Novenko, E., Ramezani, E., Röpke, A., Shumilovskikh, L., Tanţău, I., Tonkov, S., 2018. Pollen-derived biomes in the eastern mediterranean-Black Sea-Caspian-Corridor. J. Biogeogr. 45 (2), 484–499.
Maslin, M.A., Li, X.S., Loutre, M.F., Berger, A., 1998. The contribution of orbital forcing to the progressive intensification of Northern Hemisphere glaciation. Quat. Sci. Rev. 17 (4–5), 411–426.
Maslin, M.A., Ridgwell, A.J., 2005. Mid-Pleistocene revolution and the 'eccentricity myth'. Geol. Soc., Lond., Spec. Publ. 247 (1), 19–34.
Matevski, V., Čarni, A., Avramovski, O., Juvan, N., Kostadinovski, M., Košir, P., Marinšek, A., Paušič, A., Šilc, U., 2011. Forest Vegetation of the Galičica Mountain Range in Macedonia, p. 200. Ljubljana.
Matzinger, A., Schmid, M., Veljanoska-Sarafiloska, E., Patceva, S., Guseska, D., Wagner, B., Müller, B., Sturm, M., Wüest, A., 2007. Eutrophication of ancient Lake Ohrid: global warming amplifies detrimental effects of increased nutrient inputs. Limnol. Oceanogr. 52 (1), 338–353.
Matzinger, A., Spirkovski, Z., Patceva, S., Wüest, A., 2006. Sensitivity of ancient Lake Ohrid to local anthropogenic impacts and global warming. J. Great Lakes Res. 32, 158–179.
Panagiotopoulos, K., 2013. Late Quaternary Ecosystem and Climate Interactions in SW Balkans Inferred from Lake Prespa Sediments.. PhD Thesis Universität zu Köln, p. 195.
Panagiotopoulos, K., Böhm, A., Leng, M.J., Wagner, B., Schäbitz, F., 2014. Climate variability over the last 92 ka in SW Balkans from analysis of sediments from Lake Prespa. Clim. Past 10 (2), 643–660.
Peterse, F., Van Der Meer, J., Schouten, S., Weijers, J.W.H., Fierer, N., Jackson, R.B., Kim, J.-H., Sinninghe Damsté, J.S., 2012. Revised calibration of the MBT–CBT paleotemperature proxy based on branched tetraether membrane lipids in surface soils. Geochem. Cosmochim. Acta 96, 215–229.
Polunin, O., 1980. Flowers of Greece and the Balkans - A Field Guide, p. 692. Oxford.
Popovska, C., Bonacci, O., 2007. Basic data on the hydrology of lakes Ohrid and Prespa. Hydrol. Process. 21 (5), 658–664.
Postigo-Mijarra, J.M., Morla, C., Barrón, E., Morales-Molino, C., García, S., 2010. Patterns of extinction and persistence of arctotertiary flora in Iberia during the quaternary. Rev. Palaeobot. Palynol. 162 (3), 416–426.
Prentice, I.C., Cramer, W., Harrison, S.P., Leemans, R., Monserud, R.A., Solomon, A.M., 1992. Special paper: a global biome model based on plant physiology and dominance, soil properties and climate. J. Biogeogr. 117–134.
Prentice, I.C., Guiot, J., Huntley, B., Jolly, D., Cheddadi, R., 1996. Reconstructing biomes from palaeoecological data: a general method and its application to European pollen data at 0 and 6 ka. Clim. Dyn. 12, 185–194.
Pross, J., Koutsodendris, A., Christanis, K., Fischer, T., Fletcher, W.J., Hardiman, M., Kalaitzidis, S., Knipping, M., Kotthoff, U., Milner, A.M., Müller, U.C., Schmiedl, G., Siavalas, G., Tzedakis, P.C., Wulf, S., 2015. The 1.35-Ma-long terrestrial climate archive of Tenaghi Philippon, northeastern Greece: evolution, exploration, and perspectives for future research. Newsl. Stratigr.
Ravazzi, C., Rossignol Strick, M., 1995. Vegetation change in a climatic cycle of early Pleistocene age in the leffe basin (northern Italy). Palaeogeogr. Palaeoclimatol. Palaeoecol. 117 (1–2), 105–122.
Reille, M., 1992. Pollen et Spores d' Europe et d' Afrique du Nord, p. 520. Marseille.
Reille, M., 1995. Pollen et Spores d' Europe et d' Afrique du Nord (Supplement 1), p. 327. Marseille.
Reille, M., 1998. Pollen et Spores d' Europe et d' Afrique du Nord (Supplement 2), p. 521. Marseille.
Repeta, D.J., Gagosian, R.B., 1982. Carotenoid transformations in coastal marine waters. Nature 295 (5844), 51.
Russell, J.M., Hopmans, E.C., Loomis, S.E., Liang, J., Sinninghe Damsté, J.S., 2018. Distributions of 5- and 6-methyl branched glycerol dialkyl glycerol tetraethers (brGDGTs) in East African lake sediment: effects of temperature, pH, and new lacustrine paleotemperature calibrations. Org. Geochem. 117, 56–69.
Sadori, L., Koutsodendris, A., Panagiotopoulos, K., Masi, A., Bertini, A., Combourieu-Nebout, N., Francke, A., Kouli, K., Joannin, S., Mercuri, A.M., Peyron, O., Torri, P., Wagner, B., Zanchetta, G., Sinopoli, G., Donders, T.H., 2016. Pollen-based paleoenvironmental and paleoclimatic change at Lake Ohrid (south-eastern Europe) during the past 500 ka. Biogeosciences 13 (5), 1423–1437.
Sánchez Goñi, M.F., Cacho, I., Turon, J.L., Guiot, J., Sierro, F.J., Peypouquet, J.P., Grimalt, J.O., Shackleton, N.J., Grimalt, J., Shackleton, N., 2002. Synchroneity between marine and terrestrial responses to millennial scale climatic variability during the last glacial period in the Mediterranean region. Clim. Dyn. 19 (1), 95–105.
Sinopoli, G., Masi, A., Regattieri, E., Wagner, B., Francke, A., Peyron, O., Sadori, L., 2018. Palynology of the last interglacial complex at Lake Ohrid: palaeoenvironmental and palaeoclimatic inferences. Quat. Sci. Rev. 180, 177–192.
Suc, J.P., 1984. Origing and evolution of the Mediterranean vegetation and climate in Europe. Nature 307 (5950), 429–432.
Suc, J.-P., Combourieu-Nebout, N., Seret, G., Popescu, S.-M., Klotz, S., Gautier, F., Clauzon, G., Westgate, J., Insinga, D., Sandhu, A.S., 2010. The Crotone series: a synthesis and new data. Quat. Int. 219 (1–2), 121–133.
Svenning C., J., 2003. Deterministic Plio-Pleistocene extinctions in the European cool-temperate tree flora. Ecol. Lett. 6 (7), 646–653.
Tallis, J.H., 1991. Plant Community History: Long-Term Changes in Plant Distribution and Diversity, p. 398. London.
Toti, F., 2015. Interglacial vegetation patterns at the Early-Middle Pleistocene transition: a point of view from the Montalbano Jonico section (Southern Italy). Alpine Mediterr. Quat. 28 (2), 131–143.
Tzedakis, P.C., 2007. Seven ambiguities in the Mediterranean palaeoenvironmental narrative. Quat. Sci. Rev. 26 (17–18), 2042–2066.
Tzedakis, P.C., Hooghiemstra, H., Pälike, H., 2006. The last 1.35 million years at Tenaghi Philippon: revised chronostratigraphy and long-term vegetation trends. Quat. Sci. Rev. 25 (23–24), 3416–3430.
Tzedakis, P.C., Lawson, I.T., Frogley, M.R., Hewitt, G.M., Preece, R.C., 2002. Buffered tree population changes in a quaternary refugium: evolutionary implications. Science 297 (5589), 2044–2047.
Tzedakis, P.C., Margari, V., Hodell, D.A., 2015. Coupled ocean–land millennial-scale changes 1.26 million years ago, recorded at Site U1385 off Portugal. Global Planet Change 135, 83–88.
Vogel, H., Wagner, B., Zanchetta, G., Sulpizio, R., Rosén, P., 2010. A paleoclimate record with tephrochronological age control for the last glacial-interglacial cycle from Lake Ohrid, Albania and Macedonia. J. Paleolimnol. 44 (1), 295–310.
Van Der Wiel M., A., Wijmstra A., T., 1987. Palynology of the 112.8–197.8 m interval of the core Tenaghi Philippon III, Middle Pleistocene of Macedonia. Rev. Palaeobot. Palyno. 52 (2), 89–117.
Vogel, H., Meyer-Jacob, C., Thöle, L., Lippold, J.A., Jaccard, S.L., 2016. Quantification of biogenic silica by means of Fourier transform infrared spectroscopy (FTIRS) in marine sediments. Limnol Oceanogr. Methods 14 (12), 828–838.
Volkman, J.K., Barrett, S.M., Blackburn, S.I., 1999. Eustigmatophyte microalgae are potential sources of C_{29} sterols, C_{22}–C_{28} *n*-alcohols and C_{28}–C_{32} *n*-alkyl diols in freshwater environments. Org. Geochem. 30 (5), 307–318.
Wagner, B., Wilke, T., Krastel, S., Zanchetta, G., Sulpizio, R., Reicherter, K., Leng, M.J., Grazhdani, A., Trajanovski, S., Francke, A., Lindhorst, K., Levkov, Z., Cvetkoska, A., Reed, J.M., Zhang, X., Lacey, J.H., Wonik, T., Baumgarten, H., Vogel, H., 2014. The SCOPSCO drilling project recovers more than 1.2 million years of history from Lake Ohrid. Sci. Drill. 17, 19–29.
Wagner, B., Vogel, H., Francke, F., Friedrich, T., Donders, T., Lacey, J., Leng, M., Regattieri, E., Sadori, L., Wilke, T., Zanchetta, G., Albrecht, C., Bertini, A., Combourieu-Nebout, N., Cvetkoska, A., Giaccio, B., Grazhdani, A., Hauffe, T., Holtvoeth, J., Joannin, S., Jovanovska, E., Just, J., Kouli, K., Kousis, I., Koutsodendris, A., Krastel, S., Leicher, N., Levkov, Z., Lindhorst, K., Masi, A.,

Melles, M., Mercuri, A.M., Nomade, S., Nowaczyk, N., Panagiotopoulos, K., Peyron, O., Reed, J.M., Sagnotti, L., Sinopoli, G., Stelbrink, B., Sulpizio, R., Timmermann, A., Tofilovska, S., Torri, P., Wagner-Cremer, F., Wonik, T., Zhang, X., 2019. Mediterranean winter rainfall in phase with African monsoon during past 1.36 million years. Nature 573, 256–260.

Weber, Y., De Jonge, C., Rijpstra, W.I.C., Hopmans, E.C., Stadnitskaia, A., Schubert, C.J., Lehmann, M.F., Sinninghe Damsté, J.S., Niemann, H., 2015. Identification and carbon isotope composition of a novel branched GDGT isomer in lake sediments: evidence for lacustrine branched GDGT production. Geochem. Cosmochim. Acta 154, 118–129.

Weijers, J.W.H., Schouten, S., Spaargaren, O.C., Sinninghe Damsté, J.S., 2006. Occurrence and distribution of tetraether membrane lipids in soils: implications for the use of the TEX_{86} proxy and the BIT index. Org. Geochem. 37 (12), 1680–1693.

Weijers, J.W.H., Schouten, S., Van Den Donker, J.C., Hopmans, E.C., Sinninghe Damsté, J.S., 2007. Environmental controls on bacterial tetraether membrane lipid distribution in soils. Geochem. Cosmochim. Acta 71 (3), 703–713.

Whittaker, R.H., 1972. Evolution and measurement of species diversity. Taxon 21 (2), 213–251.

Wilke, T., Schultheiß, R., Albrecht, C., Bornmann, N., Trajanovski, S., Kevrekidis, T., 2010. Native *Dreissena* freshwater mussels in the Balkans: in and out of ancient lakes. Biogeosciences 7 (10), 3051–3065.

Zanni, M., Ravazzi, C., 2007. Description and differentiation of *Pseudolarix amabilis* pollen Palaeoecological implications and new identification key to fresh bisaccate pollen. Rev. Palaeobot. Palynol. 145 (1–2), 35–75.